The SAASR pattern (Structure of Abundance Across a Species

Range): synthesis, evidence and mechanisms

Brian McGill

Dept of Fisheries and Wildlife
Michigan State University
East Lansing, MI 48824
Phone: (517) 353-2927
Fax: (520) 432-1699
Email: mail@brianmcgill.org

Running head: SAASR pattern

Abstract

There is enormous variation in abundance across the range of a species. This variation does not appear to be randomly structured. In this paper I explore the details of structure of abundance across a species range (SAASR). I review the history of this pattern and show that it is deeply rooted in the history of ecology. Some claim that abundance follows a Gaussian or normal pattern across the range of the species. But many reject the claim of a Guassian SAASR. I suggest a consensus position that I call the peak-and-tail SAASR. I then test the assertions of the peak-and-tail SAASR using the North American Breeding Bird Survey (BBS). I demonstrate that while some aspects of the Gaussian SAASR are false (especially the centeredness of peak abundance), the weaker peak-and-tail SAASR is a good description of the SAASR in birds of North America. I explore possible mechanisms underlying the SAASR, taking three previously proposed mechanisms and developing them into quantitative models. I also add a fourth model. I produce predictions that can be empirically tested. No single model explains the peak-and-tail SAASR, but in combination, these models provide a good basis for understanding the SAASR. I conclude by showing that the SAASR pattern has important implications for both basic and applied ecology.

Keywords: species' range, macroecology, SAASR pattern, abundance, spatial patterns

Introduction

Macroecology deals with relationships at large scales between variables such as abundance, body size, and range size (Brown 1995). Of these variables, range size is perhaps the hardest to measure and hence range size has arguably played a lesser role relative to other macroecological variables. The two main patterns recognized in macroecology (Brown 1995, Gaston and Blackburn 2000) relating to range size are a positive correlation between range size and abundance and a roughly lognormal distribution of range sizes (Brown 1995, Brown et al. 1996, Gaston 2003). However the availability of GIS techniques and large scale census efforts has led to an increased ability to study species ranges, and a resultant resurgence of interest in the properties of species ranges (Brown et al. 1996, Gaston 2003), building on earlier efforts that were necessarily more data-limited (Rapoport 1982, Hengeveld 1990). In this paper I explore in detail a pattern with a long tradition but for which only now are we beginning to have access to sufficient data to explore the pattern rigorously.

Specifically, if one examines many sites scattered across the range of a single species, one will observe enormous variation in abundance. Moreover, this variation is spatially non-random. There is clear structure in the variation of abundance. I call this pattern the SAASR (structure of abundance across a species range) pattern. Despite the seeming importance of this pattern (argued in detail at the end of this paper), the SAASR pattern has received relatively little attention compared to many macroecological patterns. In a book dedicated to exploring patterns related to species ranges, Gaston devotes only 20 pages to the SAASR pattern. Hopefully, as GIS methods and large scale census projects become more common, this pattern will receive the attention it deserves.

The SAASR, being a study of the relationship between species ranges and abundances at large spatial scales, is an example of a macroecological pattern. The macroecological program involves two steps: 1) finding large-scale patterns and 2) finding the mechanisms behind the patterns. In the first half of this paper, I attempt to define precisely the nature of the SAASR pattern. I summarize previous thinking on the nature of the SAASR pattern, suggest a tenable description of the SAASR, and provide extensive evidence that this description is accurate. In the second part of this paper, I explore various mechanisms that might cause the observed SAASR pattern.

History of the SAASR pattern

The appreciation of systematic variation in the abundance of species across large ranges must have been known to the first peoples who moved easily across the scales of species ranges, perhaps the first sailors of the Mediterranean or Nile. Nevertheless, like so much of ecology, the first known written discussion of this phenomenon seems to have come from Charles Darwin (1859):

> "In looking at species as they are now distributed over a wide area, we
> generally find them tolerably numerous over a large territory, then
> becoming somewhat abruptly rarer and rarer on the confines, and
> finally disappearing".

This quote describes the Gaussian curve quite well — a plateau, a sharp drop, and then a very low tail of abundance.

Many pioneers of ecology also discussed this pattern. Grinnell (1904) mentions rates of increase, not abundance, but his mention of "intra-competition" suggests that he sees the two as concordant:

"The center of distribution of any animal is where the greatest rate of

increase is. … In a wide-ranging species … subcenters of distribution will

arise at points which prove to be more favorable … From each of these

new centers of distribution there will be a yearly radiating flow of

individuals into the adjacent country, so as to escape intra-competition at

any one point."

Shelford's (1931) "law of toleration" deals primarily with the edges of ranges. He

suggested that the range limits of a species are set by its ability to tolerate various

environmental factors. But his diagram (his Figure 5), clearly depicts the abundance as

being highest in the center and decreasing to the edges. Gause specifically described the

shape of the SAASR as a normal or Gaussian curve shape and fit the mathematical form

of a Gaussian curve to data (1930, 1932). However, note that his curves are plots of

abundance vs. an *environmental factor* (such as temperature), rather than spatial position.

Robert Whittaker is probably the person who most popularized the Gaussian

SAASR pattern. In 1951, he presented his now famous diagrams giving abundances of

trees along a transect up a mountain. He stated, "the curves are of binomial form, with

tapered tails". The next year in a manuscript (1952) primarily dealing with insect

abundances along transects in the Great Smoky Mountains, but also presenting plant data

from the same location, he suggests that the curves are "of the binomial, Gaussian or

normal form" and cites Gause. In the same year, Brown & Curtis (1952) published their

classic analysis of community ordination in hardwood forests of Wisconsin, plotting

abundance against a "continuum index", and suggesting that the data follow a "solid

Gaussian curve, or a part of one." By "solid", the authors mean that the data actually create a scatter diagram whose upper envelope is Gaussian in shape.

In later papers Whittaker seems varied in describing the SAASR. It is binomial in Niering et al. (1963), just Gaussian in Gauch and Whittaker (1972), and both in Whittaker (1967). It might seem pedantic to track this difference in specific words, but I will propose shortly that this difference is important. Whittaker's work reached its most assertive in a paper coauthored with Gauch (Gauch and Whittaker 1972). Here they put forth five mathematically precise assertions about the behavior of abundance curves along a transect. One assertion claims that they are normal and provides explicitly the formula for a normal curve. (The other four pertain to the relative locations and heights of the peak abundances between species.)

The early work by Whittaker and Curtis & their colleagues, and certainly the mathematically explicit hypothesis in Gauch & Whittaker (1972) inspired an entire subdiscipline. It explored patterns in vegetation along a gradient and tested the continuum hypothesis (i.e. that community composition changes gradually across space). Dozens if not hundreds of gradient studies resulted. An entire conference in Uppsala (1985) represented some of the leading workers and was published in a series of papers in *Vegetatio* (1987) and as a book (Prentice and van der Maarel 1987). Some of this work was explicitly designed as an empirical test of Whittaker's mathematical hypotheses. Most results partially supported them. For example Austin (1987) found that most curves are skewed (usually towards higher temperatures). Minchin (1989) found that 45% of the species had symmetric unimodal curves, 33% asymmetric unimodal, and 22% complex. Austin (1994) suggested that a better model than a normal or Gaussian curve would be

the Beta distribution curve, $cx^{\alpha}(1-x)^{\beta}$, which can assume many shapes ranging from nearly normal to skewed unimodal to U-shaped. An active debate on the appropriate function and fitting methods continues (e.g. Austin and Nicholls 1997). But nearly all of the work on plants has consisted of measuring a transect along an environmental gradient (e.g. altitude or flood-plain to terra firma), rather than across the entire spatial extent of a species range. Perhaps this distinction has not mattered, but it is important to keep in mind.

Although the vast majority of this work was performed on plants, similar patterns have been found in animals. Shelford's (1931) "law of tolerance" is primarily directed at animals. Some of Whittaker's early work was on insects. Whittaker asserts that insects follow a binomial or normal form, although he says this same pattern "was demonstrated with far more adequate evidence" in plants from the same location. Terborgh sampled birds along an altitudinal gradient in Peru (1971). Although he focused on different questions, he clearly draws "normal" curves very similar to those of Whittaker. Hengeveld and Haeck assembled considerable evidence for this hypothesis with data covering plants, beetles and birds in Europe (1982). Much of Hengeveld & Haeck's evidence was aggregate in nature, showing an overall tendency for abundances to be higher in the center of ranges across species, although a few diagrams did show this pattern within one individual species. Jim Brown and colleagues, working primarily with the North American Breeding Bird Survey, have added considerable evidence for this proposition (Brown 1984, 1995, Brown et al. 1995, Brown et al. 1996). Enquist and colleagues (1995) showed a pattern of increased abundance at the center of range in both fossil and modern mollusks. Numerous authors in both the plant and animal literature

have pointed out that species which are rare somewhere are usually abundant somewhere else (e.g. Schoener 1987, Murray et al. 1999).

Many authors cite bird survey atlases (Robbins et al. 1986, Root 1988a, Gibbons et al. 1993, Price et al. 1995) as evidence for (e.g. Brussard 1984) or against the normal SAASR (e.g. Lawton 1996). How can different authors look at the same bird atlas and yet some claim that the data supports the normal SAASR and others claim that it rejects the normal SAASR?

Towards a synthesis – what can we truthfully say?

I believe that this difference and most of the other disagreement about this hypothesis comes from disagreement about what the normal SAASR pattern claims, rather than a deep disagreement about the actual patterns found in nature.

Both Gause (1932) and Gauch and Whittaker (1972) explicitly invoke the mathematical formula for the normal curve ($N = c \exp(-(x-\mu)^2/\sigma^2)$). This formula has several characteristics:

> **Continuity:** abundances vary in a smooth, continuous fashion

> **Peak/drop/tail**: there is a plateau of high abundance, a sharp dropoff, and long tails.

> **Unimodality**: there is only a single peak abundance

> **Centeredness**: the peak is centered

> **Symmetry**: the data is symmetric about the peak

I suggest that the peak/drop/tail characteristic is true as is the continuity characteristic within limits, but that the last three are false. Specifically, empirical data is often multimodal (Austin 1985, 1987, Minchin 1989, Lawton 1996), not centered (Blackburn

et al. 1999, Sagarin and Gaines 2002), and not symmetric (Austin 1985, 1987, Minchin 1989).

Those who declared the SAASR to be normal were aware that the last three features were incorrect. For example, Whittaker presents a great many curves that are obviously not symmetric and some of them are multimodal (Whittaker 1951, 1952, Whittaker and Niering 1964). Brown also clearly states that the SAASR may have the mode at one edge of the range and be multimodal, yet uses the term "normal." These authors have focused on the first two features. Those who reject the normal SAASR emphasized the remaining features. Rather than try to decide who is correct, I propose that ecologists who study the SAASR pattern need to choose a new term.

Is there a descriptor other than normal which would be more accurate? The normal curve is unusual in the rigidity of its shape. In contrast, binomial curves need not be symmetric or centered. Thus, binomial curves usually provide a better fit to SAASR data than the normal curve, although they still are never bimodal. The beta distribution contains more parameters and can represent an even greater variety of shapes. Thus, various authors have described the SAASR pattern as both binomial (Whittaker 1952, Niering et al. 1963) and beta (Austin 1987), but neither of these terms can describe the full range of observed patterns (e.g. two peaks with tails on both sides of the peaks). Some authors in the plant literature have gone one step further and used smoothing/local regression types of techniques (including general additive models or GAM) instead of an explicit functional form (Bio et al. 1998, Oksanen and Minchin 2002). However, using completely malleable functions loses all predictive power.

I propose that ecologists call the SAASR pattern a "peak-and-tail" structure of abundance across a range. This seems to me to be precisely the strongest statement we can accurately make. It explicitly includes features of **Continuity** and **Peak/drop/tail** but makes no statement about **Centeredness**, **Symmetry**, or **Unimodality**, all of which we know sometimes to be untrue. The "peak-and-tail" SAASR asserts that if we look at abundance across a species' range, we will see:

➢ **Continuity:** abundances vary across space in a strongly autocorrelated, somewhat smooth fashion, albeit with considerable noise.

➢ **Few Peaks:** abundances have one to a few (up to approximately 5 but usually 1-3) distinct peaks

➢ **Small Peaks:** the peaks occupy a relatively small portion of the range

➢ **High Peaks:** the peaks have abundances 2-3 orders of magnitude greater than those found in the tails

➢ **Low tails:** the tails have very low abundances (usually going down to one individual in the entire census at some site)

➢ **Large tails:** the tails occupy a large portion of the species range

➢ **Edges mostly tails:** the tails occupy a majority of the range boundary if only because the peaks are small

➢ **Transition:** peaks drop off to tails in an intermediate region

➢ **Varying steepness:** the steepness of the drop-off of the peaks (and hence the total area of the intermediate region) varies quite a bit between species.

This provides as strong a statement as I believe we can accurately make about the SAASR.

It is worthwhile to be more precise about the first claim (continuity) of the peak-and-tail pattern. Exactly how smoothly does abundance vary? The diagrams given in Whittaker (Whittaker 1951, 1952, 1960, Whittaker and Niering 1964) suggest a very smooth variation in abundance. As Jim Brown has shown, Whittaker used a great deal of smoothing on the data (1995 see his figure 4.7). In an obituary for Robert Whittaker, two of his former graduate students (Westman and Peet 1982) made an interesting statement: "Whittaker was prone to draw 'smoothed' Gaussian curves through scatters of points with an impunity that amazed and alarmed his graduate students." But in immediately adjacent sentences these authors state, "While this ran the risk of overlooking the significant anomaly, it also succeeded in isolating broad patterns which bore well the test of 'replication' from other studies" and "he nevertheless resisted the temptation to become too entranced with elegance and simplicity." In many ways, this is the age-old debate in ecology between those seeking general patterns in the face of a noisy, chaotic world vs. those who find interest in the differences (MacArthur 1972, Kingsland 1995, Lawton 1995).

If we wish to find general patterns, understanding the nature of the noise will help to identify general patterns without ignoring exceptions. I suggest there are four different models of a noisy SAASR pattern which we might constructively consider (Figure 1). Also see Gaston's figure 4.16 (2003).

1. Completel spatial randomness (CSR in geostatistical terms); each point is independent of all the others (i.e. no spatial autocorrelation).

2. Envelop model; the SAASR provides an upper envelope with abundances ranging from zero to this upper envelope. Although abundances can be

very low within the peak, on average they are higher. This is similar to Brown & Curtis' (1952) "solid normal" SAASR as well as to a proposal by Enquist et al (1995).

3. Noisy curve, the SAASR is a smooth curve with a moderate amount of noise added to it. Presumably, a smoothing or local regression technique would get something very close to the smooth SAASR curve that underlies it. Within model #3, it may also be relevant to distinguish noise due to measurement error and process noise (noise attributable to biological/environmental causes).

4. Complete deterministic smoothness - The fourth model is the extreme opposite of complete randomness.

Fortunately, attacks on the SAASR pattern because it does not follow pattern #4 (perfect smoothness) are rare. They would be of little value since all ecologists recognize that there is considerable noise in the real world. Brown et al (Brown 1995, Brown et al. 1995) explicitly consider model #1 (complete spatial randomness) and reject it through autocorrelation studies. There is little evidence that pattern #1 is true, but it is a useful as a null model. The real question is whether pattern #2 (upper envelope) or pattern #3 (noisy smooth curve) better represents reality. Pattern #2 predicts a far noisier picture of the SAASR pattern. It also raises the possibility of a different set of mechanisms that pattern #3.

Nature of and evidence for a SAASR pattern

Considerable evidence has previously been given in the literature both that the peak-and-tail pattern is true and that we cannot make stronger statements (e.g.

unimodality). In this section, I will strengthen the evidence for this conclusion about SAASR patterns by performing a thorough examination of the North American Breeding Bird Survey (Robbins et al. 1986, Price et al. 1995). Although much work on SAASR patterns has already been done using the BBS, I will take advantage of new GIS and geostatistical tools to provide more thorough quantitative evidence over a much larger pool of species (212 birds) than previously reported.

Approach and Null Models

To demonstrate the existence of a noisy peak-and-tail structure is quite difficult. To see why, look at Figure 2. Suppose the smooth line represents the "true" distribution of abundances of a species across its range. Although this data clearly supports the peak-and-tail SAASR pattern, reasonable people would disagree on how many peaks exist. One could probably find claims for 1, 2 and 3 peaks. This problem is greatly compounded when we look not at a continuous sample across space, but the discrete samples typically observed, especially when noise is added. The asterisks represent a discrete, noisy sample. The data must be smoothed to uncover the non-random spatial pattern. Depending on the degree of smoothing used, we will find 1, 2 or 3 peaks (or possibly more). The degree of smoothing is an input parameter for which there is no objective best value. Thus, the definition of the peak itself is subjective. This presents considerable challenges for testing the peak-and-tail hypothesis. Moreover, fitting multipeaked surfaces with tails (for example the sum of bivariate normal curves) is highly ill-conditioned and therefore computationally extremely difficult.

My approach is to implement a number of null hypotheses. I then calculate a number of statistics on real SAASRs, mostly spatial in nature, and on the various null

hypotheses. This provides several statistics that directly support the claims of the peak-and-tail SAASR and further allows rejection of alternative hypotheses (the null models). I use three categories of null models.

The first null model is complete spatial randomness. I take a real species range and its abundances. I then randomly reshuffle the abundances amongst the existing sample points, without regard to spatial location. I do this once for each species of bird that I include. Thus I have 212 replicates of complete spatial randomness. This represents noise pattern #1 in Figure 1.

I use a second, closely related null model: the irruption model. For it, I create about 250 lattice points with an octagonal (nearly circular) range boundary. I then randomly assign 8 points in this lattice to have an abundance of 50. I give all remaining points an abundance of 1. This is intended to model a species that has a generally low abundance but occasionally has large outbreaks of abundance in a few random places.

Another group of null models places a Gaussian function across an octagonal range. In one variation, there is no noise (pattern #4 in Figure 1). In other variations I add noise multiplicatively (i.e. $*\exp(\varepsilon)$ where $\varepsilon \sim N(0, \sigma)$ is distributed normally with variance σ). This case corresponds with pattern #3 in Figure 1. Two additional variations test the importance of location of the peak: 1) a case where the highest peak is placed on the edge of the octagonal range rather than the center, and 2) a case with two peaks equidistant from each other and from the edges.

The third set of null models is more complicated. It is based on fractal Brownian motion (fBM) studied by Mandelbrot (1982) and reviewed for ecologists by Hastings and Sugihara (1993). The colored noise used in current stochastic population dynamics

models (Steele 1985, Pimm and Redfearn 1988, Caswell and Cohen 1995, Halley 1996, Ripa and Lundberg 1996, White et al. 1996, Petchey et al. 1997, Miramontes and Rohani 1998, Ripa et al. 1998) are one-dimensional examples of fBM. Considerable evidence suggests that environmental variables such as temperature and altitude vary according to a fBM process across space (Mandelbrot and Wallis 1969, Mandelbrot 1982, Schroeder 1991). One of the desirable properties of fBM for my purposes is that fBM actually represents a group of processes that range (as a parameter, H, varies from 0 to 1) from no spatial autocorrelation (white noise) to extreme autocorrelation (random walk or Brownian motion).

Data Methods

I downloaded BBS abundance data from more than 4000 routes (Patuxent Wildlife Research Center 2001). I averaged the abundances over a five-year period (1996-2000) to minimize sampling errors and to maximize inclusions of rare birds. I then narrowed the data (a priori, i.e. prior to analysis) as follows:

> ➢ used only routes that the administrators classified as high quality for all five years (leaving 1401 routes)
>
> ➢ further eliminated 41 routes that were north of 55° latitude because these routes were in extremely sparsely sampled areas usually in lightly populated regions of Alaska.
>
> ➢ eliminated all aquatic birds because it might be expected that birds using fresh water as a primary resource would be very patchy and birds using coastlines as a primary resource would best be analyzed in a linear fashion rather than a 2-D fashion

> eliminated species whose taxonomic definition had been split or merged in the years of the BBS

> eliminated species which do not breed in the BBS area (i.e. were accidentals or casuals)

> used only species which were found at 15 or more different routes because I considered it unlikely to get good or significant spatial patterns with fewer routes

This left 305 species of landbird across 1360 routes.

I performed the analysis with this set of birds. I then also (a priori) added the restrictions that there be at least 30 routes and that the average abundance of the species across routes where the species was found be greater than 2, primarily to eliminate species rare enough to experience sampling errors. This left 212 birds. I reran the analysis. The results with 305 species and with 212 species were qualitatively extremely similar, but statistics such as r^2 were usually 0-10 percentage points (0-0.10) lower for the larger set. All subsequent results are presented based on the more limited dataset (212 species) because it gave the stronger signal, but the results do not depend on the elimination of 93 species.

BBS data is by no means perfect for the analysis of the SAASR pattern. The sampling regime allows for considerable noise in the data. However, the use of many years, many sites, and many species should reduce all errors but systematic biases. Two commonly cited examples of systematic biases are that the BBS provides indices of abundance rather than actual abundance, and there are well-documented biases towards easily observable species in the BBS data. However, the fact that I used the data only for

comparison of relative abundances within one species largely ameliorates this problem. In the end, despite its shortcomings, the BBS is still by far the most suitable today for analysis of SAASRs due to its consistency in sampling methods across a large spatial scale and for many species.

One common criticism of studies supporting the SAASR pattern is that it is rare to have abundances sampled across the entire species range (Sagarin and Gaines 2002). Although the North American BBS is probably unique in the spatial extent and detail it covers, it still suffers from this problem. To address this I coded each of the 212 species according to how much of its range fell within the BBS boundaries (basically between 55° North latitude and the border with Mexico and between the Atlantic and the Pacific). The coding was done by visual inspection of range maps of Northern hemisphere summer breeding ranges (Kauffman 1996) and was necessarily approximate. For ranges that extended beyond the region covered by Kauffman I used a variety of sources including the World Wide Web to identify the approximate range size. I coded to one of five levels (>95% of species range within BBS boundaries, >80% within boundaries, >50% within BBS boundaries, <50% within BBS boundaries, <20% of range within BBS boundaries). I repeated all analyses using three subsets of the above 212 birds with:

➢ the 92 species having at least 95% of the range included within the BBS boundaries

➢ the 140 species having at least 80% of their range included within the BBS boundaries

➢ the 184 species having at least 50% of their range included within the BBS boundaries

The statistics did not vary meaningfully between the three cases or the full subset of 212 birds. For example, average values that were on a scale of 0-1 (e.g. r or r^2) usually differed by less than 0.05 which is in most cases an order of magnitude smaller than the range of variation found within the set of 212 species. This is not surprising for two reasons. First, the subset of 212 species was selected to have a significant presence within the BBS range. Secondly, the portions of the range that are excluded from the BBS territory are random, and as will be shown below, the location of peaks in a range are also random, so on average we are not removing any particular aspect of a species range. Based on this, the results presented in the remainder of this paper use the full subset of 212 species. *Thus although an oft repeated criticism of studies of the SAASR pattern is that they usually include only parts of ranges (Sagarin and Gaines 2002, Gaston 2003), this study appropriately controlled for this problem.*

I analyzed each species one-by-one, loading the abundance at each of the 1360 routes. The latitudes and longitudes of all routes are known. I calculated a number of statistics. The details of the statistics are discussed briefly in the relevant results section and in more detail in the table legends. Some of the statistics depended purely on the distribution of the abundances, independent of the location. A number of the statistics used a Delaunay triangulation (Bailey and Gatrell 1995) and analyzed a route vs. its nearest neighbors. This tessellation was also used to calculate the convex hull, which was considered to be the species' range. Routes on this hull were defined to be the periphery. A number of statistics such as spatial autocorrelation were based on distance between routes in km along the surface of the earth. A few statistics were calculated by doing an equal area projection of the latitude and longitude. All of these calculations were

performed in Matlab version 5.1 with the mapping add-in. Source code is available from the author.

Results – Distribution of abundances

The distribution of intraspecific abundances across multiple sites in a species' range gives a hollow curve histogram (see Figure 6 for an example), very similar to the shape of the classic single-location, interspecific histogram (SAD) (Brown et al. 1995). All but one (fBM) of the null models reproduce this distribution of abundances across space (Table 1). The logseries distribution can only produce a hollow curve shape, but the empirical data and all but the fBM null model fit the logseries with a high r^2. The skew is strongly to the left on an arithmetic scale and close to zero on a logarithmic scale. For the fBM null model, the poor fit of the logseries, the lack of skew on an arithmetic scale, and the power c exponent of ≈ 1 all combine to show that the fBM generates a symmetric distribution of abundances, not a hollow curve. This is inherent in the nature of fBM since it is a Gaussian process (according to some definitions of the term). Because of the self-similar nature of fBM, it is impossible to correct this by changing the scale along one dimension (here the vertical or abundance dimension) without destroying the structure.

To talk about peaks and tails, I have arbitrarily defined a route as being a peak route (for a given species) if it is greater than 70% of the maximum observed abundance for the species on a log scale (or equivalently $\leq N_{max}^{0.7}$). Tails are similarly defined to be less than 20% of the maximum abundance on a log scale. The three claims of the peak-and-tail SAASR that peaks are rare, tails are very common, and intermediate regions are variable, are strongly supported (Table 1 and Figure 7). Peaks occur on average at only 6.7% of the sites within a species' range. The tails occupy an average of 72%, with the

size of the intermediate region having a 95% confidence interval ranging from about 5% to about 55% of the range. The relative size of the peaks and tails stems directly from the distribution of abundances. Any null model which reproduces the distribution of abundances correctly will reproduce the area of the peaks and tails well also.

Results – Continuity and smoothness

Both the normal SAASR and the peak-and-tail SAASR claim that abundances vary in a approximately smooth and continuous fashion. To test this, I calculated the Pearson correlation, r, between abundance at each route vs the average of all of its neighbors in a Delaunay tessellation (with and without log transformation). This statistic clearly supports the claim of continuity (Table 2 and Figure 8). The average neighbor correlation for log abundances is r=0.68, indicative of significant similarity between neighbors with a good degree of noise. This statistic rejects all but one null model. The correlation in abundance between neighbors (r=0.68) far exceeds that of the completely spatially random processes (Randomized & Irruption which have r≈0) and is far below the highly structured Gaussian SAASR's (which have r≈1, even when noisy). The only null model with neighbor r's close to the empirically observed structure is that of the fBM with H=0. In some ways it is not surprising that some fBM model will be close, since the parameter H spans the range from completely spatially uncorrelated to completely spatially correlated.

Another category of measures of spatial continuity exactly parallel the above results (confirming the claim of continuity in the peak-and-tail SAASR and rejecting the same null models). I measured how often a peak route was adjacent to a peak route or a peak route was adjacent to a tail route, etc. In the completely randomized model, the odds

that a peak site neighbors a peak site are exactly equal to the percentage of peak sites in the data. In the empirical data, the odds of a peak being adjacent to a peak are much higher (average 25%), than the percentage of peaks in the overall data (6.7%). Similarly, the odds of a peak being adjacent to a tail (36%) are much lower than the odds if the data were spatially random (i.e. the percentage of tails in the data = 72%). Brown et al (1995) presented very similar data.

Results – Range of abundances

The peak-and-tail SAASR claims that the peaks are much higher in abundance than the tails and that the tails can be quite low. The empirical data confirms this (see Figure 9). The ratio between the highest and lowest abundance found within a given species range averages 557 with a 95% range of (63.5-2731) and a median of 304.5. The peak cutoff level ($N_{max}^{0.7}$) averages 117 times greater than the minimum abundance with a 95% range of (28.8-412.0) and a median of 88.1. Even the lower limit for peaks ($N_{max}^{0.7}$) greatly exceeds our upper limit for tails ($N_{max}^{0.2}$), averaging a ratio of 32.5 with a 95% range of (8.4-114.0) and a median of 24.5.

All but 3 of the 212 species have the lowest possible observed abundance of 0.2 at at least one site (1 observation/5 years). The remaining three species have the next lowest possible observed abundance (0.4) at at least one site. Within the convex hull used to define the species range, it is quite common for the species not to be observed even once in five years along the entire 24.5-mile route used by the BBS. This occurs on average at 44% of the sites within the convex hull species' range (Figure 7 and Table 1).

Results – Centeredness of peaks

One of the more controversial aspects of the normal SAASR is the claim that abundances are higher in the center. This has been documented as true and given as evidence for the normal SAASR in several cases (Hengeveld and Haeck 1982, Enquist et al. 1995), while others (using different data sets), have found no evidence for this claim (Austin 1985, 1987, Blackburn et al. 1999, Sagarin and Gaines 2002). My study of the BBS data supports those who find no evidence for this pattern. In fact, the data on the position of highest abundance vs. position in range suggests that the simplest null model of Poisson random placement of the peak within the range is quite possibly true.

To test this, I calculated a statistic (see %dist in Table 3 and Figure 10) that gives the distance of the highest observed abundance from the center of the range, rescaled into units of percentage of the radius of the range (square root of the area of the range divided by π). If the peak is at the center, the value should be 0; if the peak is on the edge, the value should be 1. If the range is elliptical, this value can actually be greater than one. Using simple calculus, one can show that the average distance from the center should be 2/3 (0.667) of the radius under a null model of Poisson random spatial placement of the peak in a circular range. Calculating this same statistic for an ellipse is not analytically tractable and varies with the eccentricity of the ellipse. The fBM models exactly match this null prediction of %dist=0.667. The Randomized model was slightly larger (%dist=0.748), because this model used actual species range boundaries which were somewhat elliptical in nature. The empirical species SAASR data gave an even slightly higher value for this statistic (0.81), although the standard deviation from this statistic is large enough (0.44) with a large enough 95% range (0.19,1.99) that we should not

consider this statistically significantly different from the Randomized or even the Poisson null model. The Irruption model was also slightly larger (0.811), presumably due to the non-circular shape of the range. In contrast, in the Gaussian null models, this statistic averaged very close to zero (slightly larger when noise was large), and in the Gaussian model with the peak on the edge, this statistic averaged close to 1.

Similarly, the proportion of peaks and tails found on average on the perimeter of the convex hull (range boundary) are nearly identical with the average for the range as a whole (see Figure 10 and Table 1; averages are 7.5% on the periphery vs 6.7% for peaks and 71.4% on the periphery vs 71.7% for tails), suggesting that there is no bias towards low abundances on the periphery. This also confirms the "**Edges mostly tails**" claim of the peak-and-tail SAASR —tails are more common on the periphery, but only because tails are more common over the whole range.

Another way to get at this problem is to divide the observed sites (routes) within a species range into four quartiles based on distance from the nearest point in the convex hull (range boundary). I then take the average abundance in each quartile and normalize by dividing by the average abundance for the species across its entire range. If there is a tendency for the center to have higher than average abundances, then the quartile farthest from the edge should have the highest index, becoming progressively lower towards the quartile abutting the edge. On the other hand, if peaks and tails are distributed randomly, then each quartile should have an average abundance equal to the average abundance over the whole range, giving an index of 1 in each quartile. This second scenario is what we actually observe (Figure 11). The mean abundance index for all four quartiles is

within .01 of the null value of 1. Interestingly, the center-most (inner) quartile is actually somewhat lower if we look at median instead of mean values.

Thus, in agreement with numerous authors (Austin 1985, 1987, Blackburn et al. 1999, Sagarin and Gaines 2002), we can soundly reject that birds display any propensity to have their peak abundances in the center of their range or to average higher abundances in the center. It remains to be understood why a few authors (Hengeveld and Haeck 1982, Enquist et al. 1995), have found a central tendency. Is this due to differences in the taxa they worked with or to the methods? Hengeveld & Haeck showed this result in plants, beetles, and European birds (in contradiction to my results on North American birds, Blackburn's results on European birds, and Austin & Minchin's results on plants). Additionally, Enquist et al found this pattern in mollusks while Sagarin & Gaines rejected it based on a metadata analysis covering a wide variety of organisms. Thus, it seems unlikely that this pattern varies among taxa. But I have also been unable to identify a causal difference in methods.

Results – Number of peaks

Another oft-disputed feature of the normal SAASR (Austin 1987, Minchin 1989, Lawton 1996) is the claim of unimodality (i.e. that there is one peak). As per the discussion above with regards to Figure 2, there is no way to determine objectively the number of peaks and test this claim. Several authors have pointed out that a simple visual inspection of the maps found in the Breeding Bird atlases (Gibbons et al. 1993, Price et al. 1995) disprove the claim of one peak (Maurer and Villard 1994, Lawton 1996). However, one must be careful to disentangle a surface that is rugged due to noise vs. one that is rugged due to multiple peaks (Figure 2). Here I quantify, to my knowledge for the

first time, the distribution of the number of peaks. I denoted peak sites as before (abundance greater than 70% of the maximum abundance on a log scale). I then took all such peaks for a single species and applied an agglomerative clustering algorithm based on average distance between elements in a cluster (MATLAB's cluster command with mode 'average'). I then took clusters whose average distance was greater than or equal to ¾ of the radius of the range (i.e. square root of range area divided by pi) and called them distinct peaks. These numbers are admittedly (indeed necessarily) arbitrary, but they seem to define peaks similar to my visual inspection.

The distribution of number of peaks is shown in Figure 20. The average number of peaks for a species was 2.87 with a 95% inclusion range of 1-5 and a median of 3. If we eliminate very tiny peaks (being defined as peaks containing less than 10% of the number of routes found in the largest peak for that species), then the distribution shifts slightly to the left (mean of 2.48 peaks with 95% range of 1-4 and median of 2). These tiny peaks may be due in some cases to observer error, but in others are probably biologically real and interesting. In general, one peak usually dominates, containing on average 65.8% of all the peak routes observed for that species. Thus the "Few peaks" claim of the peak-and-tail SAASR (there are a few, usually 1-5 peaks) is well supported, but the Unimodal claim of the normal SAASR (i.e. there is just one peak) is soundly rejected — 50% of the species had three or more peaks.

Results – Fitting smooth surfaces

Lacking a precise definition of a peak, I had to use indirect methods to test the claim that a peak and tail structure exists across the whole range (i.e. the peak/drop/tail claim of the normal SAASR and the general sense of the peak-and-tail SAASR). I used

two different techniques. One is based on fitting smooth functional surfaces to the data. The other is based on spatial autocorrelation analysis.

The most obvious test would be to fit a smooth surface represented by a function giving abundance (height) as a function of location. If this surface fits well, and possesses a peak-and-tail structure, then the claim would be supported. The challenge with this, is that the data is often multipeaked. Thus, it is not obvious what functional form to use.

One of the simplest forms one could try is a 2-D parabola (or quadratic surface). Depending on your perspective, this minimal function could be said to fit surprisingly well or poorly (average r^2 of 0.2; see Figure 12 and Table 4). A slightly more realistic function begins by log-transforming the data and then fitting a parabola. This corresponds to a 2-D Gaussian curve (which is the exponential of a quadratic equation). The fit improves, with an average r^2 of 0.33.

Fitting a quartic (order 4 polynomial) to log-transformed data gives a simple function that allows two peaks. This increases the average r^2 to 0.445. The quartic polynomial does contain 16 parameters, but that does not overfit the data since the average range has a mean of 625 routes and a median of 580 routes.

The r^2s for fitting simple polynomial surfaces to the data are especially meaningful in comparison to the null models. The r^2's are much higher than the random models (Randomized, Irruption), and much lower than any of the Gaussian null models (even the one with two peaks). The only null models which have r^2's of the same size as the actual species ranges are the fBM models, but very different values of H are needed to get an r^2 close to the observed r^2's for each of the 3 models (quadratic, log quadratic, and log quartic) described above.

Trying to fit the sum of multiple Gaussian curves (which is probably the closest mathematical description of the peak-and-tail model) is notoriously ill-conditioned, meaning that trying to fit such a model is computationally intensive and unreliable. My own experiences with attempting to fit the sum of 2-D Guassians to BBS data confirm this. Results arrived at by optimization routines were usually visibly inferior to sets of parameters that I could choose by visual inspection.

I was able to fit the sum of Gaussians to the empirical data with two simplifications: 1) I used only 1-D transects across space and 2) I used heuristics to start the optimization routines with a good guess and to constrain which variables they tried to optimize. In particular, I took the transect starting at the highest abundance in the whole range and running to the farthest away point on the range boundary. I took 100 evenly spaced points along this transect. The abundance used at each point was a linear interpolation of the three surrounding points in a Delaunay triangulation (MATLAB's "griddata(…,'linear')" function). This is an important point – there was no smoothing of the data, just interpolation of neighboring points. I then fit a modified Gaussian function of the form $N(x)=c \exp(-\sigma|x-\mu|^z)$. The modification is the extra parameter z (where $z=2$ in the Gaussian). This allows for more leptokurtic and platykurtic shapes and has been used as an extension of the Gaussian shape in past work in ecology (Roughgarden 1974). I then fit the modified Gaussian function to the transect abundances using a nonlinear least squares algorithm in MATLAB.

To fit the sum of two modified Gaussian functions (allowing for two peaks on the transects), I had to use heuristic methods to ensure the solution converged to a visually acceptable solution. I used a kernel-smoothing algorithm (Martinez and Martinez 2002)

to identify the location of the second largest peak. I then fixed this location and had the nonlinear optimization (least squares) algorithm optimize only the two σ and z parameters. I also used a functional form based on the maximum of the two modified Gaussian functions at any point rather than their sum.

Using this method, I got fits that looked moderately good, although often better fits still appeared possible. The resulting r^2's were quite good (average r^2=0.60 for 1 peak, 0.82 for two peaks; see Table 4 and Figure 12). However, this is clearly a case where null models are important. In particular, the spatially random models (Randomized, Irruption) had as good or slightly better fits, but when we examine the parameters of the fit, it becomes clear that the fit is good only because the modified Gaussian function can approximate a Dirac delta function (0 everywhere and infinity at a point). In fact, the parameters are quite different for the spatially random models then they are for real species' ranges. The Gaussian models again had noticeably better fits than empirical SAASRs (with r^2's close to 1.0). The fBM performed much more poorly (r^2's of 0.18-0.47 and 0.23-0.40 for one and two peaks respectively and for increasing values of H).

Thus, the combination of trying to fit variations on parabolic surfaces (which rejects the spatially random models) and trying to fit the modified Gaussian transects (which rejects the fBM), conclusively rejects all null models. Looking at the resulting shapes of the curve fits is also informative (see Figure 13 and Table 4). The average value of z is 2.54, not far from the Gaussian case of z=2, but the empirical ranges show considerable variation with some extremely leptokurtic and platykurtic cases. . We can

also see that although the irruptive model had good fits to the transects, the fits are far more leptokurtic (peaked) than the actual data (average z=7.7).

In summary, fitting various smooth functions that are related to the normal or Gaussian curve tells us several things. First, the empirical SAASR is distinct from all of the null models. Second, the r^2s are moderately high, especially when we consider that the peak-and-tail model allows for multiple peaks and we have only fit cases with one and two peaks. Thus although a purely Gaussian model does not describe the data optimally, it is not a terrible description. And addition of a second peak makes the fit better. This suggests that the general shape of the peak-and-tail model has fairly good support. Finally, the fact that such smooth functions can be fit to the data is further evidence for the reasonably smooth and continuous variation of abundances across a range.

Results - Autocorrelation

The second way in which I attempt to reveal the peak-and-tail SAASR is using spatial autocorrelation. A spatial autocorellogram (Bailey and Gatrell 1995) measures the degree of spatial autocorrelation at various distances. The horizontal axis represents distance, broken into bins (of 50 kms in this study). In this paper, I normalize the horizontal axis to range from 0-1 by dividing by the maximum observed distance. This allows for easy comparison between the models. The vertical axis is the covariance between points of the corresponding distance, divided by the variance of all points. This causes the values to vary usually from –1 to 1 in rough analogue to the Pearson correlation coefficient (i.e. r) for all pairs of points at the given distance apart. In a system with no spatial autocorrelation, the autocorrelogram is a horizontal line at r=0. A typical

null autocorrelation model for a system with spatial autocorrelation looks something like the function r(x)=exp(-cx) which starts with r=1 and fairly quickly decays to a r ≈ 0 for large x (distances), indicating high correlation between nearby points and no correlation between points far apart.

Brown and colleagues pioneered the use of spatial autocorrelograms to study the SAASR pattern (Brown et al. 1995). They suggested that the SAASR pattern typically shows a U-shape: the left edge of the U corresponds to local spatial autocorrelation (nearby sites are similar in abundance); the bottom of the U is negative which corresponds to peak-to-tail correlation; and the right side of the U is positive, corresponding to tail-to-tail (edge-to-edge) positive correlation. They give the autocorrelograms for four randomly chosen species which demonstrate this U pattern. I extend this work to look at 212 species.

The autocorrelation signatures of the null models are clear (see Figure 15, Figure 16, and Figure 14). The spatially random models are indeed a horizontal line at r=0. The Gaussian models with one peak in the center are U-shaped, as suggested by Brown and colleagues. However, the remaining two cases suggest that although the left 2/3 rds of the diagram varies little (a slash down to the right going from positive to negative), the right hand side depends on where the peaks are located and how many peaks there are. The autocorrelation for fBM is fairly complex, consisting of a slash down to the right followed by a series of oscillations. The number of oscillations decreases and the amplitude damps with increasing spatial autocorrelation (H). All of these are summarized in Figure 17.

What do the actual empirical SAASR autocorrelations look like? Figure 17 shows the average empirical SAASR autocorrelogram, and Figure 18 shows the autocorrelograms for a random sample of 40 species. There is a great deal of noise, and the noise increases as we move to the right. However, with a few very noisy exceptions, they begin with the slash down to the right (starting positive and decreasing to a statistically significant negative value. From there they vary drastically. Some return upwards to complete the U, resembling the centered, single peak Gaussian model. Others continue to decrease all the way to the right. Others return to zero and stay near zero. This agrees with the peak-and-tail structure as indicated by the various versions of the Gaussian model. The slash down-to-the-right from positive to negative is indicative of peaks and tails. The behavior on the right depends on how many peaks there are, where they are located in the range and even on the eccentricity of the range shape. Given our evidence that peaks are randomly located in the species range, the U-structure would not be expected to always occur.

Table 5 and Figure 19 gives a numerical quantification of the behavior of all 212 species. The r^2 reported indicates how well a 4th order polynomial fits the autocorrelogram (used as a simple measure of the smoothness and regularity of the autocorrelation). As can be seen in Figure 19, the vast majority of autocorrelograms had a high r^2, indicative of significant spatial structure (as well as smooth and continuous variation). Low r^2 values tend to correlate with low number of routes and hence small sample size. The left hand side has an average r=0.72, and an average middle value of –0.14 — together indicative of the slashing down-to-the-right pattern discussed above. Looking at the LT and LS columns of Table 5 we can see that the vast majority of

empirical autocorrelations have a statistically significant positive value on the left and even more are positive if we drop the requirement of statistical significance (both LT & LS measure the behavior of the three left-most points). The evidence for a negative middle is somewhat weaker, but 76% are negative. The behavior on the right shows no real pattern, averaging just r=0.08, barely above 0.

Summary of evidence for peak-and-tail SAASR

I have presented empirical evidence form the BBS which suggests that:

- ➢ abundance varies in a moderately smooth fashion across a range with a high degree of local spatial autocorrelation

- ➢ peak regions have very high abundances 2-3 orders of magnitude higher than the tails

- ➢ peaks are rare (averaging about 6% of a range) relative to tails (averaging about 70% of the range)

- ➢ the region of highest abundance is randomly placed within the range

- ➢ analysis of spatial autocorrelation and fitting of smooth functional forms suggest a peak-and-tail structure

- ➢ ranges have 1-5 (usually 2-3) peaks

In short, the normal SAASR is false if the assumptions of Unimodality and Centeredness are included, but has significant support if only the "smooth and continuous" and the "peak/drop/tail" claims are expanded into the peak-and-tail SAASR.

Moreover, I can reject all null models.

- ➢ The random patterns (Randomized, Irruption) have far too little local spatial autocorrelation (on average), are too poorly fit by 2-D smooth

surfaces, have 1-D smooth surfaces that drop far too quickly (i.e. too leptokurtic), and do not have the characteristic slash down-to-the-right autocorrelograms.

➢ The Gaussian models on average are too highly spatially autocorrelated and too well fit by 2-D and 1-D smooth surfaces. They do share the autocorrelograms' structure if multiple peaks variously located are included

➢ The fBM models are very poorly fit by 1-D and 2-D smooth surfaces, and do not have the correct distribution of abundances encountered at sites within a species. Although the fBM can be shown to be close to empirical ranges for some value of H, no one value of H causes fBM to be close to empirical data for all statistics. For example, neighbor correlation is close to that of empirical ranges for H close to 0, but fitting of smooth surfaces matches most closely when H is close to 1. Thus, there is no one H which makes fBM a good model.

The two models which perform best are the irruption and the Gaussian models (albeit requiring a high degree of noise, multiple peaks, and peaks located randomly). Both the irruption and pure Gaussian models can be argued to be extreme cases of the peak-and-tail SAASR. At one end (irruption), there are relatively many peaks of small size. At the other end (Gaussian), there is a single peak of very large size. Empirical SAASR's appear to fall on the spectrum between these extremes. At one end, species with overall low abundances (commonly found in birds of prey) or with very specific habitat requirements often exhibit a SAASR close to the irruption model. See Figure 21

for Cooper's hawk and Figure 22 for canyon wren. At the other extreme, some species come close to the Gaussian model with its single, large, centrally-located peak. See Figure 23 and Figure 24 for dickcissel and scissor-tailed flycatcher. Curnutt et al. (1996) suggest that many sparrows also fit this end of the spectrum. Most species, though, appear to fall somewhere in the middle of this spectrum. See Figure 25 for red-bellied woodpecker.

The peak-and-tail SAASR accurately describes the entire spectrum. It may be useful someday to develop measures describing the position within the spectrum of different SAASR's and to explore biological correlates (if any) of position within the spectrum.

One caveat: I have intentionally excluded shorebirds, freshwater aquatic birds and rare terrestrial birds. I do not know whether the peak-and-tail SAASR applies to these groups.

As Gaston (2003) suggests most of the evidence assembled to date on the normal or peak-and-tail SAASR has been somewhat circumstantial. Gaston (p. 146-148) lists four traditional types of evidence and identifies problems with each of them. The methods used herein address all of the problems raised by Gaston. By the use of a large number of species, by the calculation of a large number of spatial statistics indicative of peak-and-tail structure, by using data from species ranges and not gradients and by using whole species ranges, and especially by contrasting them with other null models of spatial autocorrelation, strong, rigorous evidence for the peak-and-tail SAASR may at last be at hand.

Towards mechanisms for the SAASR pattern

This paper gives a clear statement of a macroecological pattern: the SAASR follows a peak-and-tail structure. However, the ultimate goal of macroecology is not to find patterns, but to explain them (Brown and Maurer 1989, Brown 1995). Three mechanisms have been proposed to explain the peak-and-tail SAASR. To date, all three have been proposed only in verbal/conceptual models. This has made it difficult to rigorously test these mechanisms, and, as a result, none of them have been rejected or clearly favored. I will now develop more quantitative models of each of these three mechanisms and assess their success at explaining the peak-and-tail SAASR. I will also introduce a new model and assess its success.

Any successful theory of mechanism underlying the SAASR pattern must explain five features of the SAASR:

➢ Why are abundances spatially autocorrelated and not spatially independent?

➢ What causes peaks?

➢ What causes the intermediate (usually sharp) dropoffs in abundance from the peaks?

➢ What causes the tails?

➢ What causes the boundary of the range?

On one level, the causes of these patterns are obvious. Abiotic factors (temperature, moisture, etc.), biotic factors (competition, predation, parasites, prey) and disturbance regimes all vary across the species range. This must ultimately cause the vital population rates of birth, death, immigration, and emigration to vary across a species range (Randall 1982, Curnutt et al. 1996, Lawton 1996, Maurer 1999) and should lead to differences in

equilibrium abundances (Holt et al. 1997), and hence to the SAASR pattern. However, that level of causation is unsatisfying. Various authors have studied what sets range boundaries at a more interesting level of causation (for recent reviews see Gaston 1990, Brown et al. 1996, Gaston 2003), and I will not explore this further here. I will instead focus on the first four aspects of the SAASR pattern.

For each of the proposed mechanisms, I will: 1) briefly describe the concept, 2) develop a quantitative model, 3) assess whether the model shows the mechanism could produce the SAASR pattern, and 4) present evidence that supports the mechanism and suggest further tests of the mechanism.

Model 1: Physiological response

Concept

The concept of a physiological response curve suggests that some component of fitness responds smoothly and with a well-defined shape as some environmental variable varies; in other words, $W=f(E)$ where E is some environmental state such as temperature, W is a component of fitness such as survival or fecundity, and f is a functional form relating the two.

History

Gause adopted this approach in his pioneering work on the subject of SAASRs. He noted (1931) that "The problem of ecological distributions of organisms seems to be one of the least investigated problems of quantitative biology," sadly a statement as true today as it was then. Gause assembled a number of early physiological response curves (Gause 1930, 1931, 1932) to temperature, depth beneath the sea and various more

complex environmental measures. He suggested that the functional form of the response surface (i.e. f) is the bell-shaped normal function, $f(E)=\exp(-E^2)$, due to the central limit theorem (Grimmett and Stirzaker 1992). The grasshoppers studied by Gause himself (1930) do indeed show a Gaussian shape, but most of the rest of the data he assembled show little if any evidence for the tail aspect of the bell curve, showing instead just a unimodal hump.

Hengeveld and Haeck also list physiological response as a possible causal mechanism of the peak-and-tail SAASR and favor this choice over dispersal (1982). However, they do not develop a quantitative model.

Quantitative model

Gause used equilibrium population size as the measure of fitness. Unfortunately, later researchers were motivated by more physiological questions and measured other components of fitness such as fecundity or survivorship. This necessitates a second mapping function $N^*=g(W)=g(f(E))$ where N^* gives the equilibrium population size and g is a function mapping a component of fitness to an equilibrium population size. Very little is known about the shape of g(). Holt et al (1997) recently reiterated the point that fitness and equilibrium population size are strongly positively correlated, and hence there probably is some function g (albeit a noisy one). Ecologists often overlook this because the logistic equation has r (a measure of fitness, W) and K (i.e. N^*) as independent parameters. Others have also made this point (Williamson 1972, Kuno 1991). Holt et al give a simple model in which equilibrium population size is a linear function of fitness (i.e. $N^*=cW$), but there is no evidence for choosing the linear form over nonlinear forms.

Lawton also emphasized the link between the SAASR pattern and variation in r across space (1993)

Assessment of model

How well does the physiological response model, N*=g(f(E)) explain the peak-and-tail SAASR? The first feature (smooth and continuous variation in abundance) can be deduced if f() and g() are smooth functions and E varies smoothly and continuously over space. Of course E does not vary entirely smoothly, but at large scales this approximates reality.

Does the physiological response model explain the peak/drop/tail shape? This is less clear given modern evidence than Gause thought. The SAASR shape depends entirely on the shape of f and g, and in particular on the shape of f composed with g (f•g).

Physiologists have measured the shape of f in a wide variety of circumstances. But they have rarely reported a response surface (i.e. f) that is Gaussian in form. In general, a Monod/Michaelis-Menton functional response is measured to factors such as light, water and mineral nutrients (Farquhar et al. 1989, Botkin 1993, Kellomaki and Kolstrom 1994, Taiz and Zeiger 1998, Kinzig et al. 2002) and a parabolic response is measured to temperature (Birch 1953, Force and Messenger 1964, Jones 1992, Botkin 1993, Guttierez 1996, Taiz and Zeiger 1998). In addition, a few components of fitness, especially rates (e.g. rate of photosynthesis with unlimited water), demonstrate an exponential form of response curve f, often the Arrhenius equation (Ahlgren 1987, Kooijman 2000, Gillooly et al. 2002). But more realistic aggregate measures of fitness over larger (but biologically relevant) ranges of temperature show some unimodal form (Guttierez 1996, Kooijman 2000). Mechanistic models of the temperature response

usually produce an asymmetrical function (in contrast to the parabola), but still produce very sharp drops at the edges with some form of plateau in-between (Sharpe et al. 1977, Talkkari and Hypen 1996).

Based on current physiological knowledge, the shape of f contains a peak and a drop, but not a tail. The only way the physiological response theory can produce the full peak/drop/tail pattern is if the function g (i.e. the mapping from a component of fitness to equilibrium population size) somehow converts the sharp drops found in the shape of f into a tail. This is also necessary for Gause's results to be consistent with modern physiology. Unfortunately, ecologists after Gause have rarely measured N* as a component of fitness in a response curve. So, we have no idea what the shape of g is.

Supporting evidence and future tests

There are some reasons to think g might convert the sharp drop of f into a tail. When the component of fitness measured is survival, a sigmoidal response with a tail at one end is commonly observed. Mueller (1988) provides a simple, statistical reason why this might be true based on the shape of the cumulative distribution function of the normal curve. It is also interesting to note (since the exponential has a tail) that Gause (1932) reports an exponential increase in N* with increasing levels of food, even though traditional responses surfaces measuring food intake (in this case known as a Type II functional response) are Monod-shaped (Holling 1959). Finally, in a laboratory experiment, Davis and coworkers (1998) grew three species of *Drosophila* in four separate incubators set at a range of temperature designed to emulate those encountered by *Drosophila*. They measured equilibrium population sizes along the cline, and N* seems to show "tail-like" behavior although it is difficult to tell with only four points

along the cline. All of this evidence hints that the mapping between less aggregate components of fitness and N* may generate tails.

In the end, we do not know enough today to assess the potential of the physiological response theory to explain the full SAASR shape (including the tail). More work is needed on understanding the form of g (or in directly measuring N* as a function of environmental gradients). However, it seems that the Monod and parabolic response surfaces are quite good at explaining the peak and rapid drop aspects of a SAASR but not the long tail. Proving this hypothesis, though, requires more work. In particular, it remains to be shown that the sharp drops are observed in the natural world at the same points in the environmental gradient that they are observed in the laboratory (i.e. in the physiological response curve).

Since climate is often invoked to explain range boundaries (MacArthur 1972, Root 1988b), and I have just discussed climate as a possible cause of the SAASR, it is perhaps worth noting that two other mechanisms commonly invoked to explain range boundaries are unviable as complete explanations of the SAASR pattern. In particular metapopulations (Prince and Carter 1981, Lennon et al. 1997, Holt and Keitt 2000) and competition cause the same extremely sharp drop in abundance from a reasonably stable plateau found in physiological response functions. Thus, these factors could be invoked to explain the transition zone from peak to tail, but leave no explanation for the tail

Model 2 – Dispersal

Concepts and history

This explanation proposes that the peaks are sources, and the tails are sinks (sensu Shmida and Ellner 1984, Pulliam 1988). Grinnell clearly suggested this idea in much of

his work (1904, 1922), as exemplified by the quote I gave earlier in this paper. MacArthur (1972) develops a model based on Fretwell's Ideal Free Distribution (1969) to explain at a behavioral level why species might move to less fit regions of the environment (i.e. sinks) at the scale of a species range. Pulliam (2000) shows that migration at the scale of species' ranges can create a source-sink dynamic where a species is found outside of its fundamental niche, and Lawton suggests this verbally (Lawton 1993, Lawton 1996).

A number of other workers have suggested that dispersal causes the SAASR pattern without identifying the resulting source-sink dynamic. Lotka (1925, see also Maurer 1999) developed what he called the "intensity law," which suggests that populations behave like an ideal gas and expand outwards in areas where the "population pressure" is high. Hengeveld and Haeck (1981) cite diffusion as one of two possible explanations, although they tend to dismiss it. Schoener (1987) calls the peak-and-tail pattern "diffusive rarity" since the normal SAASR suggests diffusion to him. McCall (1990) suggests the "basin model" which is essentially the idea of an ideal free distribution or IFD (Fretwell and Lucas 1969) applied at the scale of a species range. Maurer devotes a significant portion of one chapter to developing Lotka's ideas (1999). Kirkpatrick and Barton (1997) show that species boundaries can be set by limits to local adaptation created by gene flow. Their model does produce equilibrium SAASRs that are roughly normal in shape, but they do this by putting in a Gaussian shaped carrying capacity as an assumption.

Quantitative model

Skellam (1951) gave the most useful model for the present purpose of predicting the shape of the SAASR with dispersal. He modeled population dynamics with dispersal, basing it on the mathematical (and physical) concept of diffusion and using reaction-diffusion equations (Grimmett and Stirzaker 1992, Turchin 1998, Case 2000, Kot 2001). Simple versions with unlimited population growth (i.e. exponential growth without a carrying capacity) and no spatial boundaries produce a Gaussian shaped distribution of abundance across space. This Gaussian curve expands across space forever, creating a traveling wave. This is untenable as a model of a SAASR, although it has proved useful in modeling range expansions (Shigesada and Kawasaki 1997, Turchin 1998). In the same paper, Skellam adds logistic growth (i.e. with a carrying capacity) and creates hard boundaries (all organisms diffusing beyond them die). This equation is often called the Fisher equation after R. A. Fisher who used a mathematically equivalent equation to describe gene flow across space (Fisher 1937). Kot (2001) gives an easy to follow exposition of solving the Fisher equation. The Fisher equation with hard boundaries yields a steady state solution which is unimodal, but it has extremely short tails. The solution contains a flat plateau at the carrying capacity, K, in the center and drops off quite steeply at the boundaries.

Note that the hard boundary model is equivalent to assuming a square-wave version of physiological response across an environmental gradient (i.e. $W=f(E)$ is at 0 for a while, instantaneously jumps to a constant, non-zero level for some extent, and then instantaneously jumps back to zero). In short, in order for Skellam's model to produce a

static SAASR pattern, it had to incorporate the physiological response model as an assumption. Thus, the dispersal model depends on the physiological response model.

Even by including the physiological response model, the model does not explain the SAASR (we just got back a rounded version of the square-wave function we put in with almost no tails). However, there is growing evidence that the basic assumption of the diffusion equation (that dispersal distances are Gaussian) is wrong at the scale of species ranges. Dispersal is now recognized to be heavy-tailed. This translates biologically into an excess of long distance dispersal events (Clark 1998) relative to the normal curve. This does not matter for some cases (e.g. the existence of a traveling wave seems to be robust to the exact shape of the dispersal kernel).

To test the implications of heavy-tailed dispersal on SAASR patterns, I implemented a very simple discrete model approximation to the Fisher equation. Population abundance was tracked separately at each of 100 nodes in a finite lattice. At each time step, the population at each node was calculated according to the Ricker equation. A fixed portion of each population was chosen to move with half moving to the lattice node to the left and half to the right (see for exampleCase 2000). For the long-tailed dispersion, I selected the same constant proportion to move out of each node, but the moves were not just to nearest neighbors but to all other nodes according to an exponential distribution dispersal kernel. I gave fitness (discrete intrinsic rate of increase or 'λ') a parabolic shape (unimodal hump) with a value of zero where the parabola goes negative, since $\lambda < 0$ is nonsensical. Again building the model necessitates specifying a physiological response model. I then compared traditional and heavy-tailed diffusion

while holding constant both the fitness function and the proportion of individuals moving (Figure 26).

With traditional diffusion, the model gives a plateau and then a rapid drop off in equilibrium population size to a very tiny tail that reaches zero where fitness (λ) equals zero. In contrast, with long-tailed diffusion, large tails appear which show a positive equilibrium population size in areas where $\lambda < 1$ (i.e. the definition of a sink). As a sanity check, replacing the exponential dispersal kernel with a Gaussian kernel produced the same results as the diffusion model. In short, traditional diffusion does not create creates the tails of the peaks-and-tails pattern nor does it set up a source-sink dynamic, but heavy-tailed diffusion does both.

It is possible to invoke dispersal on a variety of time scales (which was not made explicit in my model above). In some cases, the time scale may be a gradual multigenerational process (Maurer and Villard 1994). In others, a single year may suffice —neotropical migrants travel distances greater than the length of the range ever year.

Assessment of model

Thus, dispersal explains the entire peak/drop/tail SAASR. As with the physiological response model, continuity comes from the underlying continuity of response to a continuous environmental variable. Dispersal adds an additional mechanism. The mere act of dispersal increases the correlation between nearby sites. The dispersal model fully explains the peak/drop/tail pattern, but only by embedding the physiological response model.

Supporting evidence and future tests

Despite its long history, the idea that source-sink dynamics occur on the scale of species ranges is little tested. This is due to the extreme difficulty of tracking dispersal at these large scales (both spatial and number of individuals). Hopefully in the near future molecular techniques will allow a direct test of this theory (Clobert et al. 2001). Some indirect evidence exists. Maurer and Villard (1994) point out that the rate of growth of the range of the introduced European starling was most rapid in those regions where the sparrow's abundance is highest today. This suggests that the rate and degree of dispersal correlate with spatial heterogeneity in fitness. In the experiment by Davis and coworkers (1998) growing *Drosophila* in four separate incubators at various temperatures, they showed that abundances were much higher in incubators (and hence temperatures) where a given species was least fit when tubes connected the incubators. This result suggests that rescue effects (Brown and Kodric-Brown 1977) may be important across the range of environmental conditions encountered in a species range (although the spatial scale involved was much smaller).

Model 3 – Multidimensional niche

Concept and history

In 1984, Jim Brown presented a theory (1984, 1995, 1995) that explained two well-known patterns, the normal SAASR and the correlation between abundance and range size. Gaston and Blackburn call this (2000) the "niche breadth" hypothesis. The model assumes:

1. Species possess multidimensional Hutchinsonian (1957) niches

2. The match between local environmental conditions and the niche requirements for each dimension interact to set local abundance

3. Every environmental variable (e.g. temperature) has strong spatial autocorrelation but each environmental variable (e.g. temperature and moisture) behaves independently of the others (are uncorrelated)

In contrast to the physiological response model, which looks at environmental response to a single gradient, this model emphasizes that species respond to multiple environmental gradients. Involving many independent gradients allows the invocation of the central limit theorem which suggests a normal shape in the limit of many factors, regardless of the original response function shapes (i.e. f). Brown then goes on to point out that if an environmental variable abruptly changes (e.g. coastline) then the peak region of the SAASR can be close to the edge. If an environmental variable presents a multimodal pattern then the SAASR may be multimodal as well (Brown 1984).

Quantitative model

The key to making this theory more quantitative and testable is to specify whether the different dimensions of the niche interact via Liebig's law (where the most limiting factor completely controls fitness) or in an additive or multiplicative fashion (von Liebig, Lehman et al. 1975, Botkin 1993). In the first paper, Brown (1984) suggests summation $(W=f_1(E_1)+f_2(E_2)+f_3(E_3)+…)$ and provides an analogy with the additive interaction of multiple genes giving a Gaussian curve for quantitative genetics. In the same paper, he mentions simulations performed in collaboration with Sanderson and Harvey which show that this model works. These simulations incorporated simple linear environmental gradients and gave a spatial pattern similar to the normal SAASR (Jim Brown, personal

communication). In a later paper (Brown et al. 1995), the authors use multiplicative

effects of each niche (i.e. $W=f_1(E_1)f_2(E_2)f_3(E_3)\ldots$). They develop a different simulation

which unfortunately did not include a spatial component, merely producing a distribution

of abundances for a single species across many sites without spatial structure. The

authors show that various response surfaces (f) produce a lognormal-like (sigmoidal)

rank-abundance graph so long as the number of environmental factors involved exceeds

four or so. As the authors note, multiplying random variables should produce a lognormal

distribution by the central limit theorem. But the authors also note that for the number of

niche-dimensions explored, only certain combinations of parameters give the sigmoidal

rank-abundance graph.

 To explore the effects of additive vs. multiplicative models and of parameters

such as the number of niche dimensions in a spatially explicit context, I ran my own

simulations. These simulations proceeded as follows:

1. I created a rectangle measuring an arbitrary 20x20 units

2. I created D separate lines randomly across this space to represent the D
   environmental gradients corresponding to the D dimensions of the niche.
   The lines were generated by choosing a random point and then choosing a
   random orientation (angle) of the line.

3. I randomly generated the niche width of the species for each of the D
   dimensions by taking the absolute value of a random normal variable with
   a width (standard deviation) of σ (i.e. nichewidth$_i$ ~ $|N(0,\sigma)|$). The units of
   σ are arbitrary units of length and are important only in relation to the size
   of the grid (20x20).

4. At many points organized in a lattice, I calculated the distance of the point from each of the D gradient lines and then divided by the nichewidth$_i$ for that gradient.

5. I used this distance from each line (scaled by nichewidth) to calculate fitness based on one of two physiological response curves:

    a. the formula for a parabola centered over the line with a maximum height of one and with roots (fitness hitting zero) occurring nichewidth$_i$ units away from the line. Outside of the roots (i.e. more than nichewidth$_i$ units away from the line) fitness was a small value (0 or 0.1)

    b. the formula for a Gaussian normal curve with a height of one over the line and the inflection point of most rapid decrease of fitness (i.e. σ) occurring at one nichewidth$_i$ units away from the line.

6. I added or multiplied together the fitness accrued from each of the D dimensions at each lattice point in space.

7. The resulting fitness surface was plotted as a 3-D surface.

The source code for this Monte Carlo simulation is a short routine in MATLAB and is included in an appendix.

Assessment of model

I observed the following results:

1. With the right parameter values, all four models {additive, multiplicative} X {Gaussian, parabolic} can produce approximately normal-like SAASR patterns (Figure 27).

2. The average nichewidth parameter, σ, is vital. If σ is small relative to the average distance between lines, then the resulting pattern is merely a series of ridges running in different directions. Presumably, a highly skewed distribution of nichewidth$_i$ which produced an excess of small nichewidth's (e.g. lognormal) would have similar effects, although I did not test this idea.

3. Brown found a need for at least four niche dimensions, D. My model showed this requirement only for the additive model. With fewer than about four peaks, the additive model merely produces ridges. This shortcoming was lessened if the niche widths were all set to the same constant value, rather than being sampled from a normal distribution. The multiplicative model produces normal-like SAASRs with any number of niche dimensions, D (down to just 2).

4. The results vitally depended on the independence of the directions of the lines in the additive model. When, by chance most of the lines were roughly parallel, no peak was produced (again just a series of ridges). This assumption may be the weakest assumption in biological terms, as many environmental factors are correlated. The theory may be saved because the real-world gradients tend to go in two general directions: East-West (precipitation) and North-South (temperature), leading to the intersection of at least two lines.

5. The summation model generally produced much more rugose surfaces with many peaks in comparison with the product model. The summation

model also produced an insufficient amount of tail compared to empirically observed SAASRs.

6. The multiplicative parabolic model depends heavily on the fitness value assigned to points more than nichewidth$_i$ units away from the center. If the value is zero, then the scale, σ, must be nearly as large as the grid (20), otherwise, every point is almost always at least nichewidth$_i$ units away from at least one line, and the resulting fitness is zero everywhere. Thus the multiplicative parabolic model depends on either having a non-zero value assigned to faraway points (for which there is not much biological justification), or requires very large values of σ. This translates biologically into the statement that most species can tolerate (in the absence of competition) the whole range of environmental values encountered across an entire continent for individual niche dimensions. The multiplicative parabolic model can produce multiple peaks under some conditions.

In summary, the simulations suggest that Brown's niche-width hypothesis can explain the full SAASR pattern. Again spatial autocorrelation comes from the combination of smooth changes in environmental variables and smooth physiological response functions. The central limit theorem produces the peak/drop/tail pattern, but uses the physiological response model as an assumption.

Supporting evidence and future tests

This model is difficult to test due to its explicit use of many factors. Generally, the multiplicative models seem more robust, which is also the model generally favored on

empirical evidence (Lehman et al. 1975, Botkin 1993). Assuming the multiplicative model is correct, then the nichewidth needs to be large (relative to the size of a continent, see point number 6 above). We do not know if this is true, since almost no one has measured nichewidth (measured as a linear distance). Similarly, the independence of multiple environmental gradients also needs to be assessed. If the SAASR of species are driven by just two perpendicular gradients (e.g. moisture and temperature), then Brown's theory collapses to be the same as the physiological response theory.

Model 4 - Tradeoffs

Concept and history

I propose a fourth model that might explain the peak-and-tail SAASR pattern. Unlike the multidimensional niche model, this model requires only a single environmental gradient. Unlike the physiological response model, this model incorporates the idea that physiological constraints within an organism lead to tradeoffs among different components of fitness. MacArthur (1972) suggested that limits to environmental tolerance set northern range boundaries (in the Northern hemisphere), while southern range boundaries are set by being competitively inferior to the less environmentally tolerant species found towards the tropics. To my knowledge, this paper is the first time this model has been extended to explain not just the edges of ranges but the normal SAASR pattern in abundance within the range. Unlike all other proposed models, this model allows for the importance of biotic factors (interspecific interactions) as they change along a gradient.

Although one can imagine other components of fitness being involved, I extend MacArthur's ideas here. In particular, I model a tradeoff between survival due to

environmental tolerance vs. fecundity due to competitive dominance and the resulting greater food intake. Imagine a species at the center of its range. As a species moves to a harsher environment (e.g. northward and colder), it becomes less tolerant of the harsher (for the species) environment and its survival rate goes down. As the species moves towards a more benign environment, its survival rate will continue to go up. Allocation of energy and resources to environmental tolerance comes at the cost of competitive ability. One clear example was found by Loehle (1998), who compared coniferous trees and showed that both within a species and between species freezing tolerance trades off with relative growth rate (advantageous for growing tall quickly and competing for light). Thus, at the relatively harsh edge of its range, a species will have relatively more energy allocated to competitive ability than those species whose ranges are centered in even harsher climes, and will be competitively dominant. Conversely, at the relatively benign end of its range, it will have relatively more energy allocated to environmental tolerance than other species whose ranges are centered further into the benign environment and it will be competitively inferior. This tradeoff between environmental tolerance and competitive ability in closely related species is well-known, well-documented, and seems to be quite common (Connell 1961, Bovbjerg 1970, Colwell and Fuentes 1975, Woodward 1975, Woodward and Pigott 1975, Nobel 1980, 1982, Randall 1982, Rosenzweig 1985, 1989, Wisheu 1998).

Quantitative model

What SAASR would we predict from this tradeoff? The most direct line of inquiry is to assemble empirically well-documented response functions into a model. Let E represent the environmental variable. Let x represent spatial position along a line.

Assume for simplicity that E is a linear function of x. In particular, without loss of generality, I will assume E=x. Let harsh conditions be found at large values of x, and benign conditions by low values of x. Let mortality be a Gompertz sigmoidal function of environmental conditions (Mueller 1988): $\mu(E)=\exp(-c_1 \exp(-c_2 E))$. Let competitive dominance, d(x), range from 0 in the most benign conditions to 1 in the most harsh conditions in a linear fashion. Let rate of food intake (i.e. energy) be represented as $I(x)=N(x)^{d(x)-1}$ similar to several other models of intake as a function of the number of individuals and/or dominance (Schwinning and Fox 1995, Stillman et al. 2000). Assume that the total number of individuals summed across all species is constant (N(x)=K). Assume that fecundity is a function of the amount of intake energy above a maintenance threshold (Beddington et al. 1976, Rees and Crawley 1989): $R_0(x)=\max(c_3(I(x)-E_{maint}),0)$. Assuming a monocarpic (semelparous) population, then fitness is survival × fecundity: $r(x)=R_0(x)*(1-\mu(x))$. Use Holt et al's model (Holt et al. 1997) which connects fitness to equilibrium population size as $N^*(x)=r(x)/u$ (where N^* is the equilibrium population size and u is the density-independent mortality factors not otherwise modeled). For a wide range of parameters (so long as mortality and dominance cross over in the same spatial region), this model gives a peak-and-tail SAASR (Figure 28).

Assessment of model

Thus, the tradeoff model explains the entire peak/drop/tail pattern. Like the other models, continuity comes from continuity of environmental variation and physiological response. Unlike the dispersal and multidimensional niche models, the tradeoff model does not assume a parabolic physiological response. Rather the tradeoff model creates the peak/drop/tail shape by combining a sigmoidal and a hyperbolic response (with each

contributing one tail). These follow directly from choosing to model mortality and food intake. Other tradeoffs might involve other response functions which might or might not produce a peak-and-tail SAASR. Conversely, we might find other tradeoffs which produce the sigmoidal and hyperbolic response functions. Also, note that by modeling a tradeoff, we can combine two response functions.

Supporting evidence and future tests

There are no direct tests of the tradeoff model, although there exist a few suggestive pieces of evidence. This model possesses a marked skew towards the benign environment. In one of the few studies of directionality of skew in SAASRs, Austin (1987) surveyed Mediterranean-type vegetation and found that 17 out of 31 had a peak-and-tail SAASR pattern and were skewed towards high temperature (favorable environment), while only 7 were symmetric and 7 were low-temperature skewed. This skew to benign environments could be entirely coincidental, but it is suggestive. One very good example of how this mechanism of trade-off in components of fitness can produce a normal SAASR along a gradient is given by Randall (1982) (although Randall's diagrams do not show tails). Randall examined the abundance of a moth (*Coleophora alitcolella*) along an altitudinal gradient and found it displayed a normal SAASR (although he does not reference this literature or use these terms). Careful study determined that the abundance pattern was driven by an increase in paratization at lower altitudes and a decrease in food availability (seed capsules of a rush) at higher altitudes (see especially his figure 15). In this case, the trade-off is between two biotic components of fitness (parasitization and food), rather than the particular tradeoff that I suggested above. Possibly many different pairwise tradeoffs in distinct components of fitness along

a single environmental gradient can explain the SAASR pattern for different species and different gradients. In particular, it is likely that variation in biotic interactions across a gradient are important, something not accommodated in a pure physiological response model. More work like Randall's would provide a strong test of this model.

Assessment of the four mechanisms

Gause (1931) said of the SAASR pattern, "In general terms, the explanation is simple, although it is doubtful if the full story is understood in detail for any species of organism". As the above material indicates, even in general terms, the picture probably is not as simple as Gause thought. However, we are now at a point where we can give a slightly more complicated explanation of the general terms of the mechanism of the SAASR pattern. I started this section on mechanisms by describing four features of the SAASR pattern which a mechanism needed to explain:

> ➤ Why are abundances spatially autocorrelated and not spatially independent?
>
> ➤ What causes peaks?
>
> ➤ What causes the intermediate (usually sharp) dropoffs in abundance from the peaks?
>
> ➤ What causes the tails?

All four models generated continuity through the continuity of environmental variation and physiological response. The dispersal model also suggests that dispersal will connect sites and provide autocorrelation.

A parabolic physiological response function explains the peak and drop features, either directly, or by inclusion in a more complicated model (dispersal, multidimensional

niche). The tradeoffs model also explained the peak and drop features by physiological response, but used a combination of specialized response curves.

In a significant shortcoming, the simplest and oldest model (physiological response) does not produce tails (unless the mapping from fitness (W) to equilibrium population size (N*), i.e. g, generates tails). The dispersal model produces tails (which are population sinks) by rather directly pasting tails onto the parabolic physiological response via heavy-tailed dispersal. The multidimensional niche model creates tails through a more complicated mechanism: the central limit theorem. The tradeoff model creates tails by invoking two specialized physiological responses that already have tails (the sigmoidal curve and the hyperbolic curve).

In summary, some form of physiological response produces continuity, and the peak and drop portions of the peak-and-tail SAASR. But the physiological response model does not produce the tails. Thus, physiological response appears to be a necessary mechanism for producing SAASRs, but not a sufficient mechanism. Physiological response must be supplemented to produce tails. I have shown mathematically that at least four mechanisms can produce tails: dispersal, tradeoff, multidimensional niches, and certain forms of the g function. Which one is correct?

We do not know which of these mechanism produces tails in real species' ranges. I have suggested tests for all four mechanisms that might ultimately decide. It is also possible that all four factors are involved in creating tails. Some evidence exists supporting each mechanism. Ecologists have a long history of trying to reduce every question to a single explanation (Kingsland 1995), but many observed patterns are explained by multiple, complementary factors. The SAASR pattern could well fall into

this category. The appropriate mixture of the above four models might even vary from species to species and from region to region within the range of one species.

Shigesada et al (1979) developed a beautiful example of a multifactored model. They model two closely related species that compete with each other in space. Each shares a preference for a particular region of space. The authors model this by a physiological response surface that is parabolic in shape. However, one species competitively dominates the other species and preempts the inferior species in the preferred area. Both species move through diffusion and through advection away from areas of low fitness. The resulting curves of equilibrium abundances across a transect (their figure 8) look very much like a peak-and-tail SAASR such as those found empirically by Whittaker.

Implications

The SAASR pattern is important to ecology for several reasons: some are basic and others are applied. Within basic ecology, a number of authors have noted that the SAASR pattern may in fact be important in explaining the processes driving several of the most well-known patterns in macroecology. For example, the interspecific local species abundance distribution (SAD) is an extremely old, well-known and important pattern in ecology (Whittaker 1965, Tokeshi 1993, Brown 1995, Gaston and Blackburn 2000). The peak-and-tail SAASR can explain the local SAD as follows. Imagine that each species' range is placed independently in space (Poisson location of peaks) and that abundance follows a peak-and-tail SAASR. Then, at a single point in space, if we look at abundances of different species, we will effectively be sampling at random from the SAASR pattern. Because peaks are small and tails are large, and because peaks are orders

of magnitude higher than tails, this will produce the well known SAD where a few common species have abundances orders of magnitude higher than many rare (low abundance) species. This explains the equivalence shape of the interspecific local SAD and the intraspecific spatial SAD (e.g. see Figure 6). So, if we find the mechanisms for the SAASR pattern and hence intraspecific variation in abundance across space, then we have explained the interspecific local SAD. Explaining the local SAD has been a central preoccupation of ecologists (Preston 1962, May 1975, Pielou 1975, Harte et al. 1999, Dewdney 2000, Hubbell 2001), with most explanations focusing on interspecific local processes. The SAASR explanation finds the mechanism in the opposite direction – intraspecific, large-scale spatial processes. Numerous authors have independently noticed the connection between the SAD and SAASR. Brown et al (1995) and Enquist et al (1995) describe this qualitatively. Gauch and Whittaker (1972), Hengeveld et al (1979) and McGill and Collins (McGill and Collins 2003)have all developed analytical models demonstrating the validity of this connection. Using Monte Carlo simulations, McGill and Collins show that the model is quite robust to minor deviations in assumptions (e.g. replace the normal curve by a multipeaked asymmetrical curve given by the sum of three Gumbel distributions and replace completely independent placement of species ranges by a slight clustering in the spatial placement of different species ranges). Also, McGill and Collins empirically tested this theory using the North American Breeding Bird Survey (Robbins et al. 1986, Price et al. 1995). They showed that two variables explained 87% of the variance (i.e R^2) in rank abundance in local communities. These two variables are: 1) the height of the nearest peak and 2) the distance to the nearest peak (average of 682 km so this is autocorrelation at the scale of the species range, i.e. the SAASR pattern).

McGill and Collins also show that the SAASR pattern can provide an explanation for the correlation between range size and abundance. Brown (1984), going in the reverse direction, started with this correlation and developed the multidimensional niche theory to explain the SAASR pattern. McGill and Collins' also show how the SAASR pattern can explain the distribution of ranges sizes. This distribution of range sizes suffices to explain the species area relationship (SPAR) at large scales (scales greater than 10^4 km^2 for birds), an idea also independently developed by others (Leitner and Rosenzweig 1997, Maurer 1999, Allen and White 2003).

Thus, the SAASR pattern can provide an explanation for a number of the most famous patterns in macroecology. This makes understanding the SAASR pattern vitally important to basic ecology.

The SAASR pattern also has major implications for conservation biology. Specifically, the strong, non-random variation in abundance across a species' range (2-3 orders of magnitude in birds) has important implication for conservation as first noted by Brown et al (1995). Presence/absence data of many species is commonly combined together to identify areas likely to contain many species which can then be prioritized for conservation in a process known as GAP analysis (Scott et al. 1993). GAP analysis deals only with presence/absence data, explicitly rejecting any data on abundance (Jennings et al. 1997). This is worrying since the abundance in the tails is quite low, and the risk of extinction increases greatly with low abundance (MacArthur and Wilson 1967, Goel and Richter-Dyn 1974, Gilpin and Soule 1986, Pimm et al. 1988). Reserves in the tails may be orders of magnitude less valuable than reserves in the peaks. Where possible, conservation studies need to move beyond mere presence and absence data.

The main reason for using presence/absence data instead of abundance data is the time and dollar cost of obtaining data comparable to that found in the BBS. Conservation planning should not be put on hold in cases where abundance data is unavailable. But the SAASR pattern may also contain a partial solution to difficulties in obtaining abundance data across an entire species range. In particular, understanding the degree of structure in the peak-and-tail SAASR pattern suggests that, if we are clever, we ought to be able to identify peaks and tails with much less sampling effort than previously thought. This will allow for the development of more sophisticated models that predict not just presence of a species but its abundance in a hypothetical reserve (e.g. Bolger et al. 1997), and ultimately its extinction risk.

Thinking about the mechanisms behind the SAASR pattern has even further implications for conservation biology. Lomolino and Chanell (1998) have shown that when species are reduced to a very small fraction of their range, the remnant population is usually found in a peripheral region largely due to chance processes (Channell and Lomolino 2000). The patterns presented in this paper give conflicting interpretations of their work. On the one hand, given the random location of peaks, these retractions may still be towards peaks, contrary to the interpretation most often given to these results. On the other hand, given the proportion of peaks to tails and a model of chance contagion processes, this suggests that most often (but not always) the species will be found in a tail region. The exact effect of relict populations being in tails depends on which mechanisms are dominant in creating the tail. If one of the physiological response, multidimensional niche, or tradeoff models cause tails, then this implies that remnant populations will be in very poor habitat for the species. If the dispersal model plays a large role in creating the

tails, then this has even more dire implications. Reserves located in the tails are sinks under this theory. Once the sources (peaks) have been destroyed, the sinks are doomed to extinction in the long run (Lawton 1993, Lawton 1996).

Summary

This paper started with a review of the literature on SAASRs. I demonstrated that the idea in a qualitative fashion is quite old. Starting in the 50's and accelerating into the 70's, ecologists started to describe the pattern more quantitatively as "normal". Much of the evidence at this time came not from transects across a species range but across an environmental gradient. As the pattern began to be called normal, others began to object, because the normal curve is a special curve and thus makes the "normal" SAASR a strong statement.

I proposed that about half the features implied by the normal SAASR are true and about half are false. This suggests that progress on the study of the SAASR pattern will be greater if we can more accurately name the pattern. I suggested the peak-and-tail SAASR as a more accurate description, and I list the assumptions of the peak-and-tail SAASR.

I then tested these features using the North American breeding bird survey. All of the features of the peak-and-tail SAASR were shown to be true, even in comparison to several null models of spatial autocorrelation. The idea of abundance being highest in the center was also shown to be false.

Finally, I explored three previously proposed theories and one new theory of the mechanisms which underlie the peak-and-tail SAASR pattern. I made the existing models more quantitative which led to predictions and possible tests. The physiological response

mechanism seems central but probably needs to be supplemented by another mechanism to produce tails. Much work is needed to test which mechanisms are actually involved.

The SAASR explains many well-established, important patterns of macroecology, and empirical tests support the SAASR mechanism. The SAASR also has strong implications for conservation biology. The SAASR emphasizes the importance of using abundance data instead of presence/absence data and provides a means to reduce the costs of predicting abundance across space. The SAASR pattern also warns conservationists to worry about which mechanisms cause tails when reserves are located in tails.

Acknowledgements

References

Ahlgren, G. 1987. Temperature functions in biology and their applications to algal growth constants. Oikos **49**:177-190.

Allen, A. P., and E. P. White. 2003. Effects of range size on species-area relationships. Evolutionary Ecology Research **5**:493-499.

Austin, M. P. 1985. Continuum concept, ordination methods, and niche theory. Annual Review of Ecology and Systematics **16**:39-61.

Austin, M. P. 1987. Models for the analysis of species' response to environmental gradients. Vegetatio **69**:35-45.

Austin, M. P., and A. O. Nicholls. 1997. To fix or not to fix the species limits, that is the ecological question: Response to Jari Oksanen. Journal of Vegetation Science **8**:743-748.

Austin, M. P., A. O. Nicholls, M. D. Doherty, and J. A. Meyers. 1994. Determining Species Response Functions to an Environmental Gradient by Means of a Beta-Function. Journal of Vegetation Science **5**:215-228.

Bailey, T. C., and A. C. Gatrell. 1995. Interactive spatial data anlaysis. Longman Scientific & Technical, Harlow, England.

Beddington, J. R., M. P. Hassell, and J. H. Lawton. 1976. The components of arthropod predation: II the predator rate of increase. Journal of Animal Ecology **45**:165-185.

Bio, A., R. Alkemade, and A. Barendregt. 1998. Determining alternative models for vegetation response analysis: a non-parametric approach. Journal of Vegetation Science **9**:5-16.

Birch, L. C. 1953. Experimental background to the study of the distribution and abundance of insects. I. The influence of temperature, moisture, and food on the innate capacity for increase of three grain beetles. Ecology **34**:698-711.

Blackburn, T. M., K. J. Gaston, R. M. Quinn, and R. D. Gregory. 1999. Do local abundances of British birds change with proximity to range edge? Journal of Biogeography **26**:493-505.

Bolger, D. T., T. A. Scott, and J. T. Rotenberry. 1997. Breeding bird abundance in an urbanizgin landscape in coastal Southern California. Conservation Biology **11**:406-421.

Botkin, D. B. 1993. Forest dynamics; an ecological model. Oxford University Press, Oxford.

Bovbjerg, R. V. 1970. Ecological isolation and competitive exclusion in two crayfish (Orconectes Virilis and Orconectes Immunis). Ecology **51**:225-236.

Brown, J. H. 1984. On the relationship between abundance and distribution of species. American Naturalist **124**:255-279.

Brown, J. H. 1995. Macroecology. Univ of Chicago Press, Chicago.

Brown, J. H., and A. Kodric-Brown. 1977. Turnover rates in insular biogeography: Effect of immigration on extinction rates. Ecology **58**:445-449.

Brown, J. H., and B. A. Maurer. 1989. Macroecology: the division of food and space among species on continents. Science **243**:1145-1150.

Brown, J. H., D. H. Mehlman, and G. C. Stevens. 1995. Spatial variation in abundance. Ecology **76**:2028-2043.

Brown, J. H., G. C. Stevens, and D. M. Kaufman. 1996. The geographic range: size, shape boundaries, and internal structure. Annual Review of Ecology and Systematics **27**:597-623.

Brown, R. T., and J. T. Curtis. 1952. The upland conifer-hardwood forests of Northern Wisconsin. Ecological Monographs **22**:217-234.

Brussard, P. F. 1984. Geographic patterns and environmental gradients: the central-marginal model in drosophila revisited. Annual Review of Ecology and Systematics **15**:25-64.

Case, T. J. 2000. An illustrated guide to theoretical ecology. Oxford University Press, New York.

Caswell, H., and J. E. Cohen. 1995. Red, White, and Blue: environmental variance spectra and coexistence in metapopulations. Journal of Theoretical Biology **176**:301-316.

Channell, R., and M. V. Lomolino. 2000. Trajectories to extinction: spatial dynamics of the contraction of geographical ranges. Journal of Biogeography **27**:169-179.

Clark, J. S. 1998. Why trees migrate so fast: confronting theory with dispersal biology and the paleorecord. American Naturalist **152**:204-224.

Clobert, J., E. Danchin, A. A. Dhondt, and J. D. Nichols, editors. 2001. Dispersal. Oxford University Press, Oxford.

Colwell, R. K., and E. R. Fuentes. 1975. Experimental studies of the niche. Annual Review of Ecology and Systematics **6**:281-310.

Connell, J. H. 1961. The influence of interspecific competition and other factors on the distribution of the barnacle Cthamalus stellatus. Ecology **42**:710-723.

Curnutt, J. C., S. L. Pimm, and B. A. Maurer. 1996. Population variability of sparrows in space and time. Oikos **76**:131-144.

Darwin, C. 1859. On the origin of species. Clows and Sons, London.

Davis, A. J., J. H. Lawton, B. Shorrocks, and L. S. Jenkinson. 1998. Individualistic species responses invalidate simple physiological models of community dynamics under global environmental change. Journal of Animal Ecology **67**:600-612.

Dewdney, A. K. 2000. A dynamical model of communities and a new species-abundance distribution. The Biological Bulletin **198**:152-165.

Enquist, B. J., M. A. Jordan, and J. H. Brown. 1995. Connections between ecology, biogeography, and paleobiology: relationship between local abundance and geographic distribution in fossil and recent molluscs. Evolutionary Ecology **9**:586-604.

Farquhar, G. D., S. v. Caemmerer, and J. A. Berry. 1989. A biochemical model of photosynthetic CO_2 assimilation in leaves of C3 species. Planta **149**:79-90.

Fisher, R. A. 1937. The wave of advance of advantageous genes. Annuals of Eugenics **7**:355-369.

Force, D. C., and P. S. Messenger. 1964. Fecundity Reproductive Rates + Innate Capacity for Increase of 3 Parasites of Therioaphis Maculata (Buckton). Ecology **45**:706-&.

Fretwell, S. D., and H. L. J. Lucas. 1969. On territorial behavior and other factors influencing habitat distribution in birds. Acta Biotheoretica **19**:16-36.

Gaston, K. J. 1990. Patterns in the geographical ranges of species. Biological Reviews **65**:105-129.

Gaston, K. J. 2003. The structure and dynamics of geographic ranges. Oxford University Press, Oxford.

Gaston, K. J., and T. M. Blackburn. 2000. Pattern and Process in Macroecology. Blackwell Science, Ltd, Oxford.

Gauch, H. G. J., and R. H. Whittaker. 1972. Coencline simulation. Ecology **53**:446-451.

Gause, G. F. 1930. Studies on the ecology of the Orthoptera. Ecology **11**:307-325.

Gause, G. F. 1931. Influence of ecological factors on the size of populations. American Naturalist **65**:70-76.

Gause, G. F. 1932. Ecology of populations. The Quarterly Review of Biology **VII**:27-46.

Gibbons, D. W., J. B. Reid, and R. A. Chapman. 1993. The new atlas of breeding birds in Britain and Ireland: 1988-1991. Poyser, London.

Gillooly, J. F., E. L. Charnov, G. B. West, V. M. Savage, and J. H. Brown. 2002. Effects of size and temperature on developmental time. Nature **417**:70-73.

Gilpin, M. E., and M. E. Soule. 1986. Minimum Viable Populations: Processes of Species Extinction. Pages 19-34 *in* M. E. Soule, editor. Conservation Biology: The science of scarcity and diversity. Sinauer Associates, Sunderland, MA.

Goel, N. S., and N. Richter-Dyn. 1974. Stochastic models in biology. Academic Press, New York.

Grimmett, G. R., and D. R. Stirzaker. 1992. Probability and random processes. Clarendon Press, Oxford.

Grinnell, J. 1904. The origin and distribution of the Chestnut-backed Chickadee. The Auk **21**:364-378.

Grinnell, J. 1922. The role of the "accidental". The Auk **39**:373-380.

Guttierez, A. P. 1996. Applied population ecology: a supply-demand approach. John Wiley & Sons, New York.

Halley, J. M. 1996. Ecology, evolution and 1/f-noise. Trends in Ecology and Evolution **11**:33-37.

Harte, J., A. P. Kinzig, and J. Green. 1999. Self-similarity in the distribution and abundance of species. Science **284**:334-336.

Hastings, H. M., and G. Sugihara. 1993. Fractals: a user's gide for the natural sciences. Oxford University Press, Oxford.

Hengeveld, R. 1990. Dynamic Biogeography. Cambridge University Press, Cambridge.

Hengeveld, R., and J. Haeck. 1981. The distribution of abundance II Models and implications. Proceedings of the Koninklijke Nederlandse Akadamie Van Wetenschappen C **84**:257-284.

Hengeveld, R., and J. Haeck. 1982. The distribution of abundance I. Measurements. Journal of Biogeography **9**:303-316.

Hengeveld, R., S. A. L. M. Kooijman, and C. Taillie. 1979. A spatial model explaining species-abundance curves. Pages 337-347 *in* J. K. Ord, G. P. Patil, and C. Taillie, editors. Statistical distributions in ecological work. International Co-operative Publishing House, Fairland, Maryland.

Holling, C. S. 1959. The components of predation as revealed by a study of small mammal predation of the European pine sawfly. The Canadian Entomologist **91**:293-320.

Holt, R. D., and T. H. Keitt. 2000. Alternative causes for range limits; a metapopulation perspective. Ecology Letters **3**:41-47.

Holt, R. D., J. H. Lawton, K. J. Gaston, and T. M. Blackburn. 1997. On the relationship between range size and local abundance: back to basics. Oikos **78**:183-190.

Hubbell, S. P. 2001. A Unified Theory of Biodiversity and Biogeography. Princeton University Press, Princeton.

Hutchinson, G. E. 1957. Concluding remarks. Cold Spring Harbor Symposia on Quantitative Biology **22**:415-427.

Jennings, M. D., B. Csuti, and J. M. Scott. 1997. Wildlife habitat relationship models: Distribution and abundance. Conservation Biology **11**:1271-1272.

Jones, H. G. 1992. Plants and microclimate: A quantitative approach to environmental plant physiology. Cambridge University Press, Cambridge.

Kauffman, K. 1996. Lives of North American Birds. Houghton Mifflin Co, Boston.

Kellomaki, S., and M. Kolstrom. 1994. The influence of climate change on the productivity of Scots pine, Norway spruce, Pendula birch and pubesecent birch in southern and northern Finland. Forest Ecology and Management **65**:201-217.

Kingsland, S. E. 1995. Modelling Nature: episodes in the history of population ecology, 2nd edition. University of Chicago Press, Chicago.

Kinzig, A. P., S. W. Pacala, and D. Tilman, editors. 2002. The functional consequences of biodiversity. Princeton University Press, Princeton, NJ.

Kirkpatrick, M., and N. H. Barton. 1997. Evolution of a species range. American Naturalist **150**:1-23.

Kooijman, S. A. L. M. 2000. Dynamic energy and mass budgets in biological systems, 2nd edition. Cambridge University Press, Cambridge.

Kot, M. 2001. Elements of Mathematical Biology. Cambridge University Press, Cambridge.

Kuno, E. 1991. Some strange properties of the logistic equation define with r and K: inherent defects or artefacts. Researches on Poulation Ecology **33**:33-39.

Lawton, J. H. 1993. Range, Population Abundance and Conservation. Trends in Ecology and Evolution **8**:409-413.

Lawton, J. H. 1995. Webbing and Wiwacs. Oikos **72**:305-306.

Lawton, J. H. 1996. Population abundances, geographic ranges and conservation: 1994 Witherby Lecture. Bird Study **43**:3-19.

Lehman, J. T., D. B. Botkin, and G. E. Likens. 1975. The assumptions and rationale of a computer model of phytoplankton population dynamics. Limnology and Oceanography **20**:343-364.

Leitner, W. A., and M. L. Rosenzweig. 1997. Nested species-area curves and stochastic sampling: a new theory. Oikos **79**:503-512.

Lennon, J. J., J. R. G. Turner, and D. Connell. 1997. A metapopulation model of species boundaries. Oikos **78**:486-502.

Loehle, C. 1998. Height growth rate tradeoffs determine northern and southern range limits for trees. Journal of Biogeography **25**:735-742.

Lomolino, M. V., and R. Channel. 1998. Range collapse, re-introductions, and biogeographic guidelines for conservation. Conservation Biology **12**:481-484.

Lotka, A. J. 1925. Elements of mathematical biology. Williams & Wilkins, New York.

MacArthur, R. H. 1972. Geographical ecology: Patterns in the distribution of species. Princeton University Press, Princeton, NJ.

MacArthur, R. H., and E. O. Wilson. 1967. The theory of island biogeography. Princeton University Press, Princeton, NJ.

Mandelbrot, B. B. 1982. The fractal geometry of nature. W. H. Freeman and Co, New York.

Mandelbrot, B. B., and J. R. Wallis. 1969. Some long-run properties of geophysical records. Water Resources Research **5**:321-340.

Martinez, W. L., and A. R. Martinez. 2002. Computational statistics handbook with MATLAB. Chapman & Hall/CRC, Boca Raton.

Maurer, B. A. 1999. Untangling ecological complexity. University of Chicago Press, Chicago.

Maurer, B. A., and M. A. Villard. 1994. Geographic variation in abundance of North American birds. Research and Exploration **10**:306-317.

May, R. M. 1975. Patterns of species abundance and diversity. Pages 81-120 *in* M. L. Cody and J. M. Diamond, editors. Ecology and evolution of communities. Belknap Press of Harvard University Press, Cambridge, MA.

McCall, A. D. 1990. Dynamic geograph of marine fish populations. University of Washington, Seattle.

McGill, B. J., and C. D. Collins. 2003. A unified theory of macroecology based on spatial and interspecific patterns of abundance. Evolutionary Ecology Research **5**:469-492.

Minchin, P. R. 1989. Montane vegetation of Mt Field massif, Tasmania: a test of some hypotheses about properties of community patterns. Vegetatio **83**:97-110.

Miramontes, O., and P. Rohani. 1998. Intrinsically generated coloured noise in laboratory insect populations. Proceedings of the Royal Society of London B **265**:785-792.

Mueller, L. D. 1988. Density-dependent population growth and natural selection in food-limited environments: the Drosophila model. American Naturalist **132**:786-809.

Murray, B. R., B. L. Rice, D. A. Keith, P. J. Myerscough, J. Howell, A. G. Floyd, K. Mills, and M. Westoby. 1999. Species in the tail of rank-abundance curves. Ecology **80**:1806-1816.

Niering, W., R. Whittaker, and C. Lowe. 1963. The Saguaro: a population in relation to its environment. Science **142**:15-23.

Nobel, P. S. 1980. Morphology, surface temperatures, and Northern limits of columnar cacti in the Sonoran desert. Ecology **61**:1-7.

Nobel, P. S. 1982. Low-temperature tolerance and cold hardening of cacti. Ecology **63**:1650-1656.

Oksanen, J., and P. R. Minchin. 2002. Continuum theory revisited: what shape are species responses along ecological gradients. Journal of Vegetation Science **157**:119-129.

Patuxent Wildlife Research Center. 2001. Breeding Bird Survey FTP site. *in*. Patuxent Wildlife Research Center - Laurel, MD.

Petchey, O. L., n. Gonzalez, and H. B. Wilson. 1997. Effects on population persistence: the interaction between environmental noise colour, intraspecific competition and space. Proceedings of the Royal Society of London B **264**:1841-1847.

Pielou, E. C. 1975. Ecological Diversity. John Wiley & Sons, New York.

Pimm, S. L., H. L. Jones, and J. Diamond. 1988. On the risk of extinction. American Naturalist **132**:757-785.

Pimm, S. L., and A. Redfearn. 1988. The variability of population densities. Nature **334**:613-614.

Prentice, I. C., and E. van der Maarel, editors. 1987. Theory and models in vegetation science. W. Junk, Dordrecht.

Preston, F. W. 1962. The canonical distribution of commonness and rarity: part I. Ecology **43**:185-215.

Price, J., S. Droege, and A. Price. 1995. The summer atlas of North American birds. Academic Press, San Diego, CA.

Prince, S. D., and R. N. Carter. 1981. Epidemic models used to explain biogeographical distribution limits. Nature **293**:644-645.

Pulliam, H. R. 1988. Sources, Sinks, and Population Regulation. The American Naturalist **132**:652-661.

Pulliam, H. R. 2000. On the relationship between niche and distribution. Ecology Letters **3**:349-361.

Randall, M. G. M. 1982. The dynamics of an insect population throughout its altitudinal distribution: Coleophora alitcolella (Lepidoptera) in northern England. Journal of Animal Ecology **51**:993-1016.

Rapoport, E. H. 1982. Aerography: geographical strategies of species. Pergammon, Oxford.

Rees, M., and M. J. Crawley. 1989. Growth, Reproduction and Population-Dynamics. Functional Ecology **3**:645-653.

Ripa, J., and P. Lundberg. 1996. Noise colour and the risk of population extinctions. Proceedings of the Royal Society of London B **263**:1751-1753.

Ripa, J., P. Lundberg, and K. Viejo. 1998. A general theory of environmental noise in ecological food webs. American Naturalist **151**:256-263.

Robbins, C. S., D. Bystrak, and P. H. Geissler. 1986. The breeding bird survey: its first fifteen years, 1965-1979. US Dept of the Interior, Fish and Wildlife Service, Washington, DC.

Root, T. 1988a. Atlas of wintering North American birds: an analysis of the Christmas Bird Count data. University of Chicago Press, Chicago.

Root, T. 1988b. Energy constraints on avian distributions and abundances. Ecology **69**:330-339.

Rosenzweig, M. L. 1985. Some theoretical aspects of habitat selection. Pages 517-539 *in* M. L. Cody, editor. Habitat selection in birds. Academic press, New York.

Rosenzweig, M. L. 1989. Habitat selection, community organization, and small mammal studies. Pages 5-21 *in* D. W. Morris, Z. Abramsky, B. J. Fox, and M. R. Willig, editors. Patterns in the structure of mammalian communities. Spec Publ Mus, Texas Tech, Lubbock.

Roughgarden, J. 1974. Species packing and the competition function with illustrations from coral reef fish. Theoretical Population Biology **5**:163-186.

Sagarin, R. D., and S. D. Gaines. 2002. The 'abundant' centre distribution: to what extent is it a biogeographical rule? Ecology Letters **5**:137-147.

Schoener, T. W. 1987. The geographical distribution of rarity. Oecologia **74**:161-173.

Schroeder, M. 1991. Fractals, chaos, and power laws: minutes from an infinite paradise? W. H. Freeman and Co, New York.

Schwinning, S., and G. A. Fox. 1995. Population-Dynamic Consequences of Competitive Symmetry in Annual Plants. Oikos **72**:422-432.

Scott, J. M., F. Davis, B. Csuti, R. Noss, B. Butterfield, C. Groves, H. Anderson, S. Caicco, F. Derchia, T. C. Edwards, J. Ulliman, and R. G. Wright. 1993. Gap Analysis - a Geographic Approach to Protection of Biological Diversity. Wildlife Monographs:1-41.

Sharpe, P. J. H., G. L. Curry, D. W. DeMichele, and C. L. Cole. 1977. Distribution model of organism developmental times. Journal of Theoretical Biology **66**:21-38.

Shelford, V. E. 1931. Some concepts of bioecology. Ecology **21**:455-467.

Shigesada, N., and K. Kawasaki. 1997. Biological invasions: theory and practice. Oxford University Press, Oxford.

Shigesada, N., K. Kawasaki, and E. Teramoto. 1979. Spatial segregation of interacting species. Journal of Theoretical Biology **79**:83-99.

Shmida, A., and S. Ellner. 1984. Coexistence of plant species with similar niches. Vegetatio **58**:29-55.

Skellam, J. G. 1951. Random dispersal in theoretical populations. Biometrika **38**:196-218.

Steele, J. H. 1985. A comparison of terrestial and marine ecological systems. Nature **313**:355-358.

Stillman, R. A., J. D. Goss-Custard, A. D. West, S. E. A. le V Dit Durell, R. W. G. Caldow, S. McGorty, and R. T. Clarke. 2000. Predicting mortality in novel environments: tests and sensitivity of a behavior-based model. Journal of Applied Ecology **37**:564-588.

Taiz, L., and E. Zeiger. 1998. Plant Physiology, 2nd edition. Sinauer Associates, Sunderland, MA.

Talkkari, A., and H. Hypen. 1996. Development and assessment of a gap-type model to predict the effects of climate change on forests based on spatial forest data. Forest Ecology and Management **83**:217-228.

Terborgh, J. 1971. Distribution of environmental gradients: theory and a preliminary interpretation of distributional patterns in the avifauna of the cordillera Vilcabamba, Peru. Ecology **52**:24-40.

Tokeshi, M. 1993. Species abundance patterns and community structure. Advances in Ecological Research **24**:111-186.

Turchin, P. 1998. Quantitative analysis of movement: measuring and modeling population redistribution in animals and plants. Sinauer Associates, Sunderland, MA.

von Liebig, J. 1862. Die Chemie in irher Anwendung auf Agricultur und Physiologie, 7e edition. F. Vieweg und Sohn, Braunschweig.

Westman, W. E., and R. K. Peet. 1982. Whittaker, Robert H (1920-1980) - The man and his work. Vegetatio **48**:97-122.

White, A., M. Begon, and R. G. Bowers. 1996. Explaining the colour of power spectra in chaotic ecological models. Proceedings of the Royal Society of London B **263**:1731-1737.

Whittaker, R. H. 1951. A criticism of the plant association and climatic climx concepts. Northwest Science **25**:17-31.

Whittaker, R. H. 1952. A study of summer foliage insect communities in the Great Smoky Mountains. Ecological Monographs **22**:1-44.

Whittaker, R. H. 1960. Vegetation of the Siskiyou mountains, Oregon and California. Ecological Monographs **30**:279-338.

Whittaker, R. H. 1965. Dominance and diversity in land plant communities. Science **147**:250-260.

Whittaker, R. H. 1967. Gradient analysis of vegetation. Biological Review **42**:207-264.

Whittaker, R. H., and W. A. Niering. 1964. Vegetation of the Santa Catalina mountains, Arizona I Ecological classification and distribution of species. Journal of the Arizona Academy of Science **3**:9-34.

Williamson, M. 1972. The analysis of biological populations. Arnold, London.

Wisheu, I. C. 1998. How organisms partition habitats: different types of community organization can produce identical patterns. Oikos **83**:246-258.

Woodward, F. I. 1975. The climatic control of the altitudinal distriubtion of Sedum rosea (L.)Scop and S. Telephium L. II The analysis of plant growth in controlled environments. New Phytologist **74**:335-348.

Woodward, F. I., and C. D. Pigott. 1975. The climatic control of the altitudinal distriubtion of Sedum rosea (L.)Scop and S. Telephium L. I Field observations. New Phytologist **74**:323-334.

Appendix 1 – MATLAB Source code for test of the Brown Niche Hypothesis

```
function testbrownclt(n,scale,bBeyond,bNicheLines)
% testbrownclt(#gradients [5],nichescale vs grid 20x20 1],
bBeyondEdges[0], bDrawNicheLines[0])
if nargin<1, n=5; end
if nargin<2, scale=1; end
if nargin<3, bBeyond=0; end
if nargin<4, bNicheLines=0; end

%generate random lines as a point and an angle
if bBeyond, spacescale=60; else spacescale=20; end
lnX=rand(1,n)*spacescale-10;
lnY=rand(1,n)*spacescale-10;
if scale>0,
    nichewidth=abs(randn(1,n)*scale);
else
    nichewidth=repmat(scale,1,n);
end
lnang=rand(1,n)*2*pi;
% calculate second point on the line
lnX2=lnX+1;
lnY2=lnY+tan(lnang);
% get slope & intercept
m=(lnY2-lnY)./(lnX2-lnX);
b=lnY-m.*lnX;
gridsize=21;
gridsize=61;
x=linspace(-10,10,gridsize);
y=linspace(-10,10,gridsize);
[X,Y,L]=meshgrid(x,y,1:n);
dist=abs((m(L).*X-Y+b(L))./sqrt(m(L).^2+1));
nw=repmat(reshape(nichewidth,[1 1 length(nichewidth)]),[gridsize
gridsize 1]);
W=(dist./nw+1).*(1-dist./nw); %parabola with zeros at dist/nw and
height of 1
parabolicmin=0;
%W=W+10;

figure;
X=squeeze(X(:,:,1));
Y=squeeze(Y(:,:,1));
subplot(2,2,1);
plotfitness(X,Y,sum(max(W,parabolicmin),3));
title('Sum');xlabel('X');ylabel('Y');
zlabel('Parabolic');
drawlines(bNicheLines,m,b,nichewidth);
subplot(2,2,2);
plotfitness(X,Y,prod(max(W,parabolicmin),3));
drawlines(bNicheLines,m,b,nichewidth);
title('Product');xlabel('X');ylabel('Y');
subplot(2,2,3);
plotfitness(X,Y,sum(exp(W),3));
drawlines(bNicheLines,m,b,nichewidth);
```

```
xlabel('X');ylabel('Y');
zlabel('Gaussian');
subplot(2,2,4);
plotfitness(X,Y,prod(exp(W),3)*1e10);
drawlines(bNicheLines,m,b,nichewidth);
xlabel('X');ylabel('Y');


function plotfitness(X,Y,Z)
surf(X,Y,Z);
%contourf(X,Y,Z);
hold on;
[c,h]=contour(X,Y,Z,[0 0]);
set(h,'LineWidth',2,'LineStyle','-.','EdgeColor','w');
colorbar;



function drawlines(bNicheLines,m,b,nichewidth)
if length(m)>5 | nichewidth>50, return; end;
if ~bNicheLines, return;end;
hold on;
x=linspace(-10,10,5);
for ln=1:length(m),
    y=m(ln).*x+b(ln);
    h=line(x,y,vector(1000,x));
    set(h,'LineWidth',nichewidth(ln)/2);
end
axis([-10, 10, -10,10]);
```

Tables

	LS mc r^2	Power r^2	Power c	Skew	LnSkw	%Peak	%Tail	%Empty
Real (n=305)	0.891	0.886	0.166	2.895	0.028	0.058	0.772	0.497
Real (n=212)	0.86	0.902	0.138	2.998	-0.18	0.067	0.717	0.44
Randomized	0.86	0.902	0.138	2.998	-0.18	0.067	0.717	0.44
Irruption	0.652	0.623	0.053	5.468	5.468	0.03	0.969	N/A
Gauss s=0	0.857	0.948	0.27	1.45	-0.04	0.099	0.688	N/A
Gauss s=0.1	0.863	0.948	0.224	1.504	-0.04	0.002	0.995	N/A
Gauss s=0.25	0.851	0.938	0.161	1.79	-0.04	0.002	0.99	N/A
Gauss s=0.5	0.825	0.908	0.091	2.925	-0.03	0.003	0.982	N/A
Gauss Pk on Edge	0.601	0.986	0.35	1.066	-0.49	0.147	0.609	N/A
Gauss 2 Peaks	0.33	0.994	0.305	1.119	-0.97	0.094	0.619	N/A
fBM H=0	-0.06	0.944	1.017	0.009	-2.93	0.11	0.108	N/A
fBM H=0.25	0.077	0.944	1.032	0.01	-2.32	0.119	0.116	N/A
fBM H=0.5	0.191	0.952	1.042	0.01	-1.82	0.142	0.142	N/A
fBM H=0.75	0.27	0.961	1.039	0.004	-1.57	0.163	0.172	N/A
fBM H=0.95	0.305	0.97	1.068	0	-1.4	0.197	0.192	N/A

Table 1 – Distribution of intraspecific abundances across observation sites (routes). This table presents summary statistics (averages across 212 replicates) for eight different statistics that describe the distribution of abundances found across a species' range, independent of any spatial patterns. **LS mc r^2** gives a mean-corrected r^2 for how well the logseries distribution fits the data. The **Power r^2** gives the same statistic for the power distribution. The **Power c** statistic gives the exponent of the cdf in the power distribution. **Skew** gives the observed skew of the distribution of abundances, while **LnSkew** gives the observed skew of log abundances. **%Peak** gives the percentage of sites (routes) that are a peak, arbitrarily defined as 70% of the maximum abundance on a log scale (i.e. $N \geq \exp(0.7*\log(N_{max}))=N_{max}^{0.7}$. **%Tail** gives the corresponding percentage of routes in the tail, arbitrarily defined as

20% of N_{max} on a log scale, i.e. . $N \leq \exp(0.2*\log(N_{max}))=N_{max}^{0.2}$. **%Empty** gives the percentage of routes within the convex hull range that had no observations of the species at the route. Empty sites are not modeled in the null models and are treated as a very low abundance (0.1 or ½ bird in 5 years) in most of the rest of the statistics. Note that the Randomized and Real (n=212) cases are identical since the Randomized null model merely spatially reshuffled the data from the same set of real species.

	NbrR	LnNbR	%PnP	%PnT	%TnP	%TnT
Real (n=305)	0.472	0.615	0.202	0.473	0.028	0.857
Real (n=212)	0.527	0.685	0.245	0.362	0.028	0.832
Randomized	0	0	0.065	0.714	0.066	0.717
Irruption	-0.01	-0.01	0.024	0.975	0.03	0.969
Gauss s=0	0.998	0.997	0.871	0	0	0.963
Gauss s=0.1	0.988	0.994	0.04	0.868	0.001	0.995
Gauss s=0.25	0.938	0.978	0.029	0.859	0.002	0.991
Gauss s=0.5	0.783	0.926	0.029	0.834	0.003	0.984
Gauss Pk on Edge	0.998	0.998	0.916	0.002	0	0.969
Gauss 2 Peaks	0.998	0.998	0.806	0	0	0.954
fBM H=0	0.537	0.48	0.234	0.034	0.035	0.232
fBM H=0.25	0.791	0.742	0.403	0.008	0.008	0.4
fBM H=0.5	0.916	0.886	0.581	0.002	0.002	0.579
fBM H=0.75	0.967	0.949	0.706	0.001	0.001	0.712
fBM H=0.95	0.983	0.971	0.778	0.001 1	0.00	0.772

Table 2 – Smooth and continuous nature of data and null models This table presents data that measures the degree of smooth, continuous change in abundance across space of the different models. **NbrR** gives the Pearson r statistic of correlation between a given site (route's abundance) and the average abundance at all of its immediate neighbors in a Delaunay triangulation, while **LnNbR** gives the identical statistic except the correlation was calculated after log transformation. **%PnP** gives the average % of nearest neighbors which are a peak given that the target site is a peak. **%PnT** gives the percentage of nearest neighbors that are tails, given that the target site is a peak, and so on (**%TnP** gives % of nearest neighbors that are peaks given that the target site is a tail).

	ACmid%	%dist
Real (n=305)	3463.0	0.843
Real (n=212)	3556.0	0.813
Randomized	4111	0.748
Irruption	416.2	0.79
Gauss s=0	350	0.028
Gauss s=0.1	350	0.085
Gauss s=0.25	350	0.131
Gauss s=0.5	350	0.167
Gauss Pk on Edge	650	0.919
Gauss 2 Peaks	350	0.62
fBM H=0	30.47	0.666
fBM H=0.25	29.35	0.694
fBM H=0.5	29.23	0.7
fBM H=0.75	30.14	0.677
fBM H=0.95	29.19	0.676

Table 3 – Statistics on distance of highest peak from center of range. The **ACmid%** statistic gives the average distance at which autocorrelation was most negative (i.e peak to tail). The numbers are only comparable within groups (i.e. first 4 models, the Gauss models, the fBM models). The **%dist** statistic describes how far the peak is from the center of the species' range as a percentage of the radius (calculated as the squareroot of the area of the convex hull divided by π); a value of 0 indicates at the center and a value of 1 indicates on the edge. In theory values greater than 1 are possible for the first 4 models which may have oblong ranges.

	Par r2	LPar r2	Lquarr2	Trns1	T1 σ	T1 z	Trns2
Real (n=305)	0.187	0.293	0.408	0.617	3.033	2.34	0.831
Real (n=212)	0.2	0.333	0.445	0.597	2.925	2.535	0.821
Randomized	0.019	0.02	0.056	0.469	2.951	7.771	0.786
Irruption	0.023	0.023	0.064	0.679	0.685	1.881	0.987
Gauss s=0	0.749	1	1	0.999	0	2.007	0.999
Gauss s=0.1	0.736	0.994	0.994	0.989	0	2.751	0.971
Gauss s=0.25	0.676	0.968	0.968	0.924	0.002	3.273	0.904
Gauss s=0.5	0.502	0.884	0.885	0.786	0.348	1.862	0.805
Gauss Pk on Edge	0.934	1	1	0.999	0	1.981	0.999
Gauss 2 Peaks	0.59	0.929	0.987	0.531	1.816	0.121	0.284
fBM H=0	0.02	0.018	0.073	0.182	0.312	0.436	0.216
fBM H=0.25	0.064	0.057	0.194	0.257	0.559	0.411	0.253
fBM H=0.5	0.112	0.104	0.348	0.358	0.697	0.484	0.294
fBM H=0.75	0.158	0.145	0.493	0.392	0.926	0.509	0.332
fBM H=0.95	0.193	0.176	0.585	0.469	0.85	0.692	0.409

Table 4 – Fitting normal curves to the models These statistics all describe fitting smooth continuous curves to the data. **Par r2** gives the proportion of variance explained by fitting a 2-D parabola (quadratic equation) to the abundances. **Lpar r2** gives the same statistic with the abundances log transformed first. Note that a parabola in log space is identical with the Gaussian normal curve. **Lquarr2** gives the goodness of fit of log transformed abundances to a quartic (4th degree) polynomial – the smallest degree that can have two peaks with tails on both edges. **Trns1** gives the r^2 for the fit of a modified Gaussian function ($N=c_1 \exp(-(|x-c_2|/\sigma)^z)$) to the 1-D transect from the point of highest abundance within the range to the farthest point along the range boundary. The two variables T1σ

and T1z gives the respective parameters in this function and are both measures of how sharp and wide the peak is. Note that z=2 is the Gaussian case. **Trns2** gives the r^2 fit for maximum of two modified Guassian functions as described in the text.

	LS	MS	RS	LT	MT	RT	Ushap	r2	u-l	u-m	u-r
Real (n=305)	0.613	0.38	0.085	0.908	0.761	0.36	0.232	0.659	0.317	-0.13	0.081
Real (n=212)	0.721	0.477	0.113	0.952	0.807	0.433	0.254	0.717	0.358	-0.14	0.112
Randomized	0	0	0	0.061	0.263	0.155	0.009	0.133	0	-0.02	0.014
Irruption	0	0	0	0.028	0.136	0.018	0.018	0.521	0	-0.02	0.067
Gauss s=0	1	1	1	1	1	1	1	0.997	0.95	-0.46	0.621
Gauss s=0.1	1	1	1	1	1	1	1	0.997	0.934	-0.46	0.611
Gauss s=0.25	1	1	1	1	1	1	1	0.997	0.856	-0.42	0.561
Gauss s=0.5	1	1	1	1	1	1	1	0.996	0.638	-0.31	0.414
Gauss Pk on Edge	1	1	0	1	1	0	0	0.999	0.957	-0.69	-0.64
Gauss 2 Peaks	1	1	1	1	1	1	1	0.998	0.966	-0.37	0.434
fBM H=0	0.028	0.183	0.061	0.849	0.311	0.141	0.004	0.878	-2.66	-0.04	-0.01
fBM H=0.25	0.33	0.301	0.084	1	0.367	0.146	0.084	0.932	-6.93	-0.07	-0.08
fBM H=0.5	0.82	0.344	0.075	1	0.481	0.117	0.047	0.955	-4.88	-0.14	-0.19
fBM H=0.75	1	0.292	0.084	1	0.415	0.084	0.061	0.976	-5.12	-0.22	-0.34
fBM H=0.95	1 0 0.33		0.08	1	0.45	0.089	0.037	0.981	-1.55	-0.26	-0.37

Table 5 –Autocorrelation structure LS indicates that the bins 3,4, & 5 on the left are statistically significantly positive. **RS** indicates that the bins 2nd, 3rd and 4th from the right are statistically significantly positive. **MS** indicates that the 3 bins centered around the lowest observed r are all statistically significantly negative. **LT** indicates a trend (bins 2,3, & 4th from the left are >0), **RT** indicates a trend on the right (bins 2nd,3rd and 4th from right are >0), and **MT** indicates that the 3 bins in the middle are all less than zero.

Figures
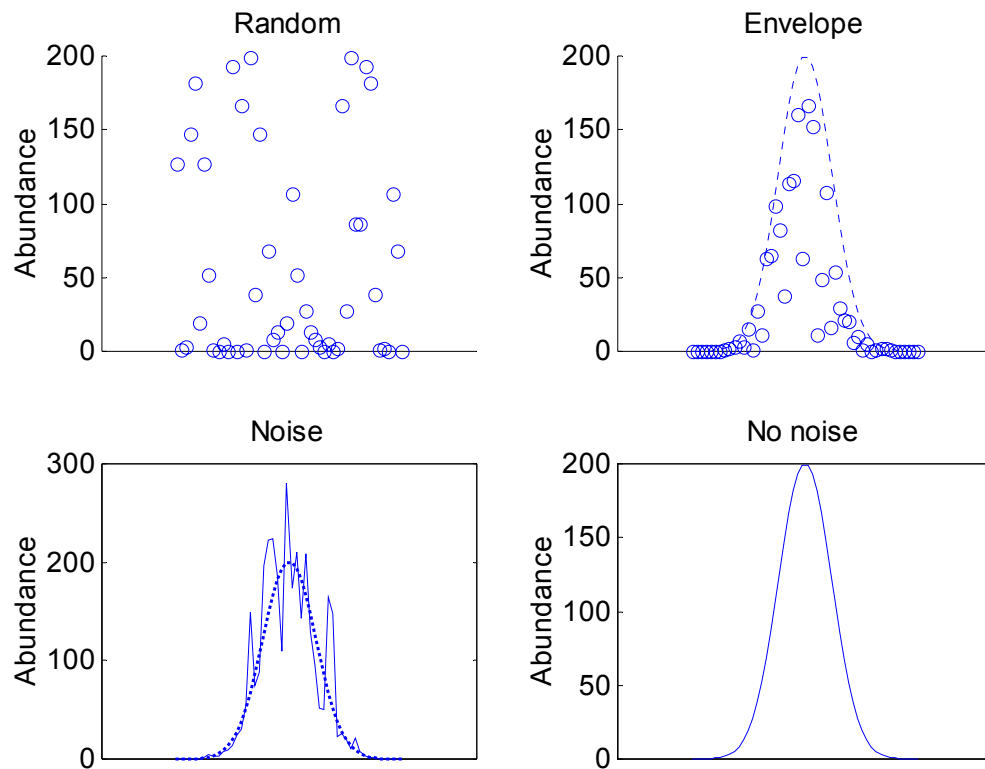
Figure 1 – Four different models of noise for SAASR. For simplicity, these examples use the Gaussian SAASR even though we know it is not precisely true. See the text for detailed descriptions.
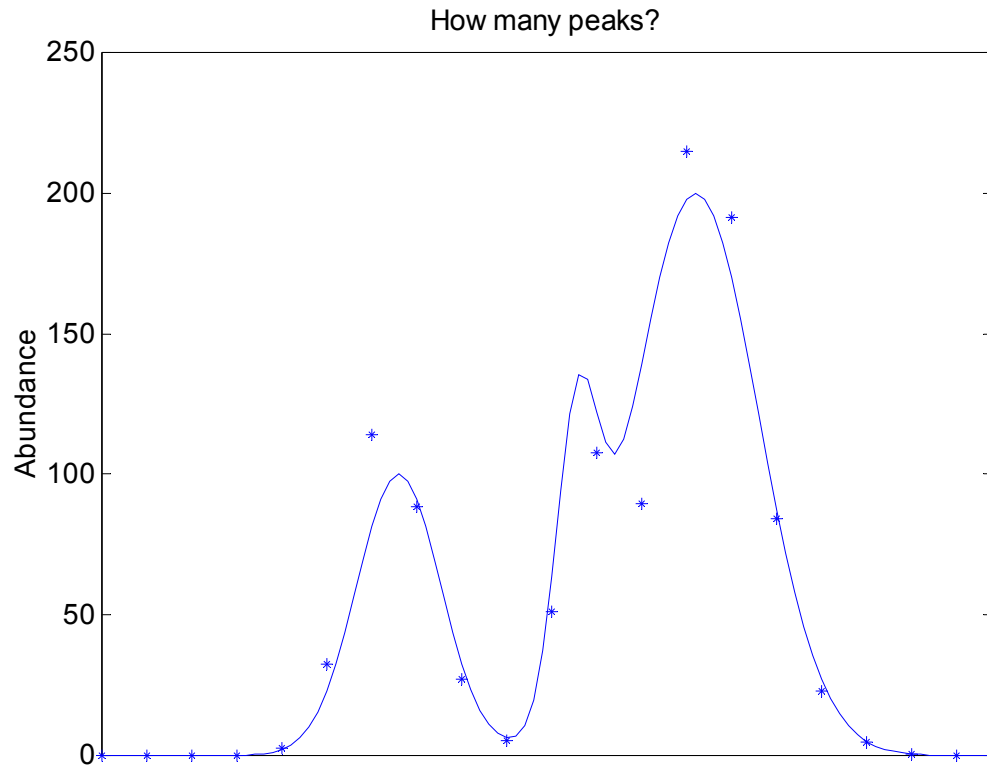
Figure 2 – Demonstration that the definition of the # peaks is subjective.

Mathematically, if we are given the smooth solid line, there is a well defined number of

peaks (where the first derivative is zero and the 2nd derivative is negative — in this case

3 peaks). In practice, for a given question we may not wish to consider all of these as true

peaks. The problem becomes even more complicated when we have only a discrete

sample from this continuous function and the sample has noise, as shown by the asterisks.
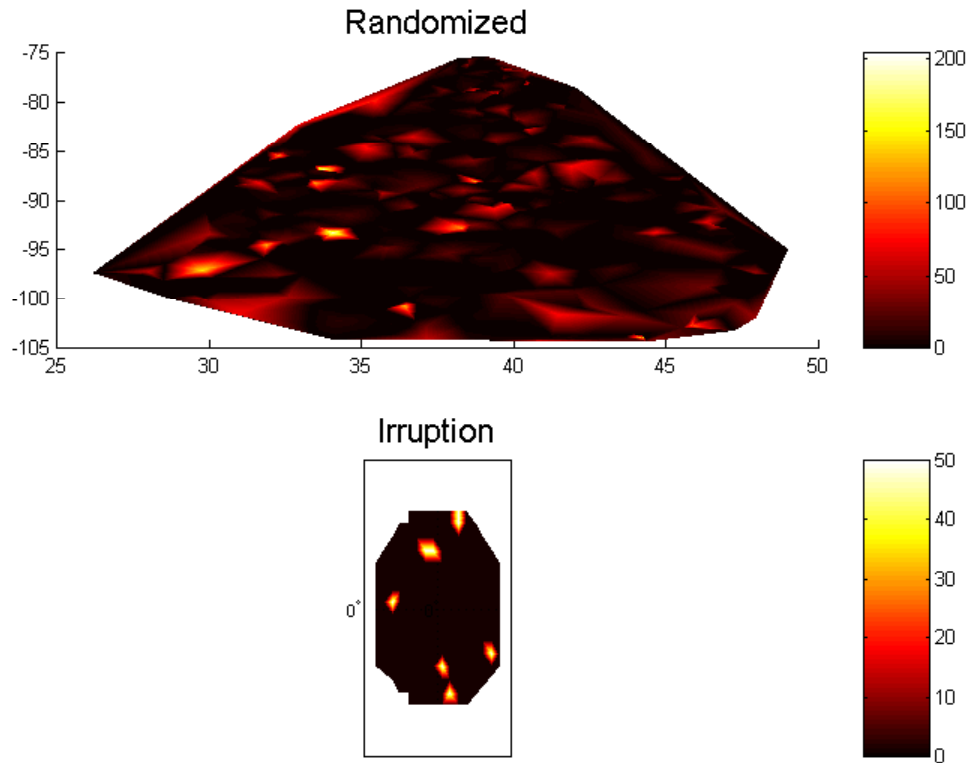
Figure 3 – Spatially random null models Two null models that are random with respect to space and show no spatial autocorrelation. The first model took empirically observed SAASR patterns and reshuffled the abundances randomly. The Irruption model, set a low abundance (N=1) everywhere, and then randomly chose 8 points to have a high (N=50) abundance.
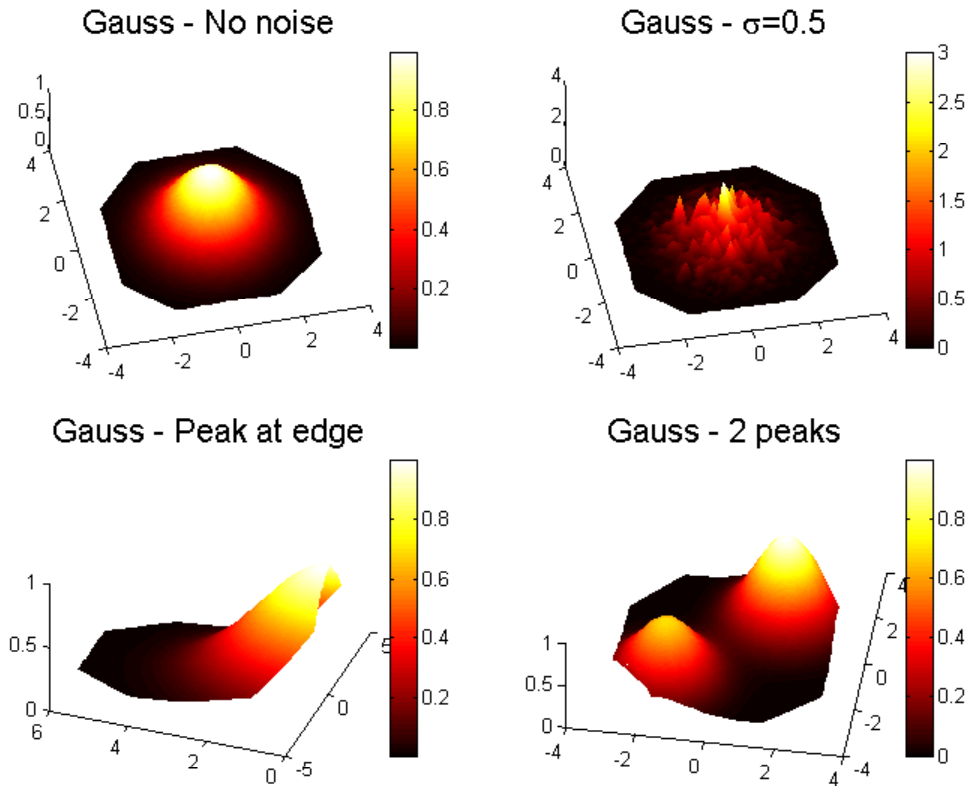
Figure 4 – Gaussian null models This diagram shows a null model based on the Gaussian bell curve across space. The simplest model is a bell curve with the peak centered. Various levels of noise, σ, were also added. Because of the effects on autocorrelation structure, I also modeled cases with the peak at the edge and with two peaks.
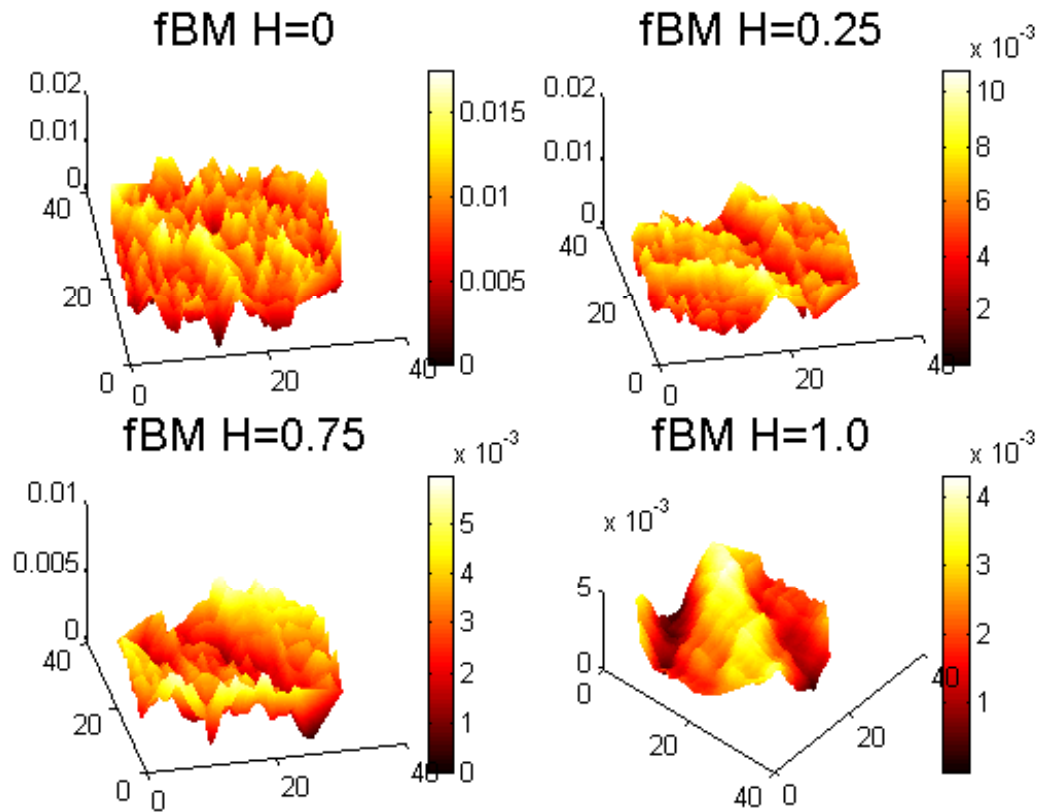
Figure 5 – fBM null model for different values of H This diagram shows samples of the randomly generated surfaces of a fractal Brownian Motion process (Mandelbrot 1982) used as null models of spatial autocorrelation. H=0 corresponds to nearly no spatial autocorrelation (white noise), while H=1 corresponds to very high local autocorrelation (random walk).
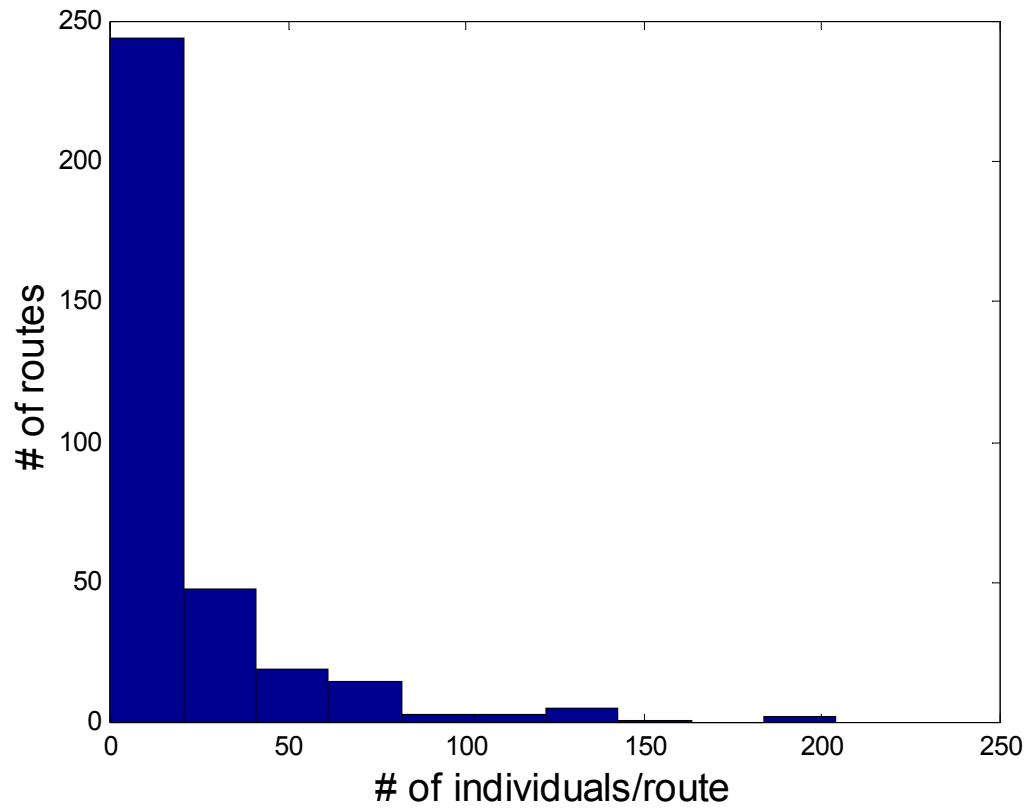
Figure 6 – Intraspecific distribution of abundances. Histogram of abundances

for the species Dickcissel over all routes where the species is observed.
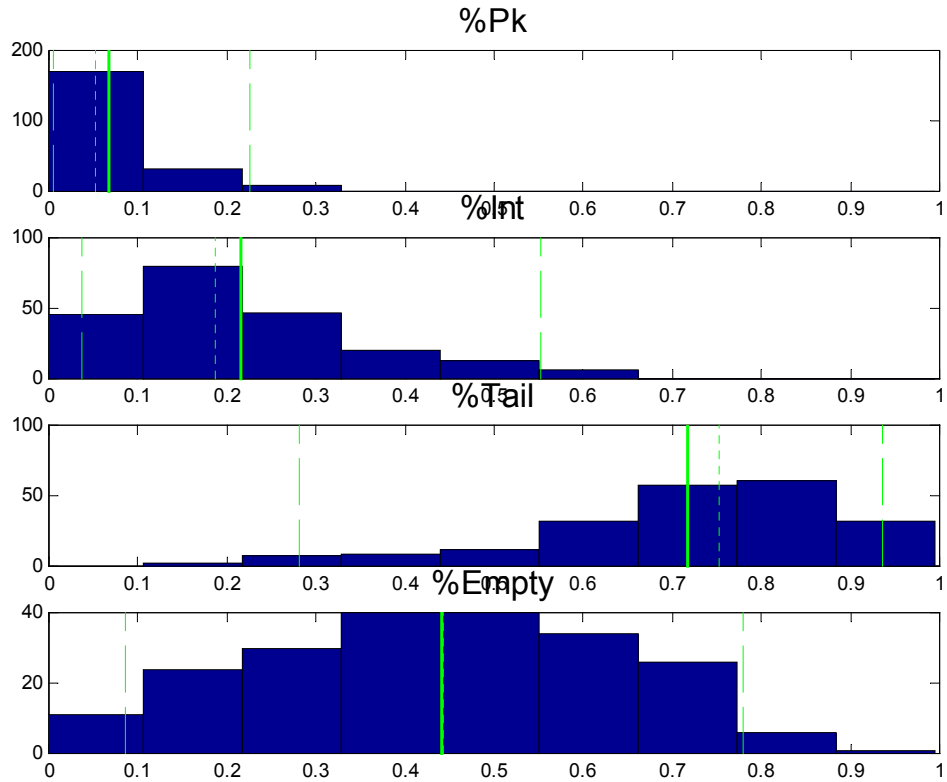
Figure 7- Distribution of area of peaks, tails and intermediate areas as a percentage of total range area for real species. This diagram shows the distribution of the proportion of a range that is classified as peak (>70% of the maximum abundance on a log scale), tail (<20% of the maximum abundance on a log scale), and intermediate (>20%, <70%). For a given species these three numbers add up to 1. The 4th graph shows the percentage of cites within the species' convex hull range at which no individuals were observed (generally treated as an abundance of 0.1 in the rest of this paper and included as a tail in this diagram). In this and all following histograms, the solid vertical bar represents the mean. The dotted vertical bar represents the median, and the two dashed vertical bars represent the 95% inclusion interval (95% of the values are inside this range).
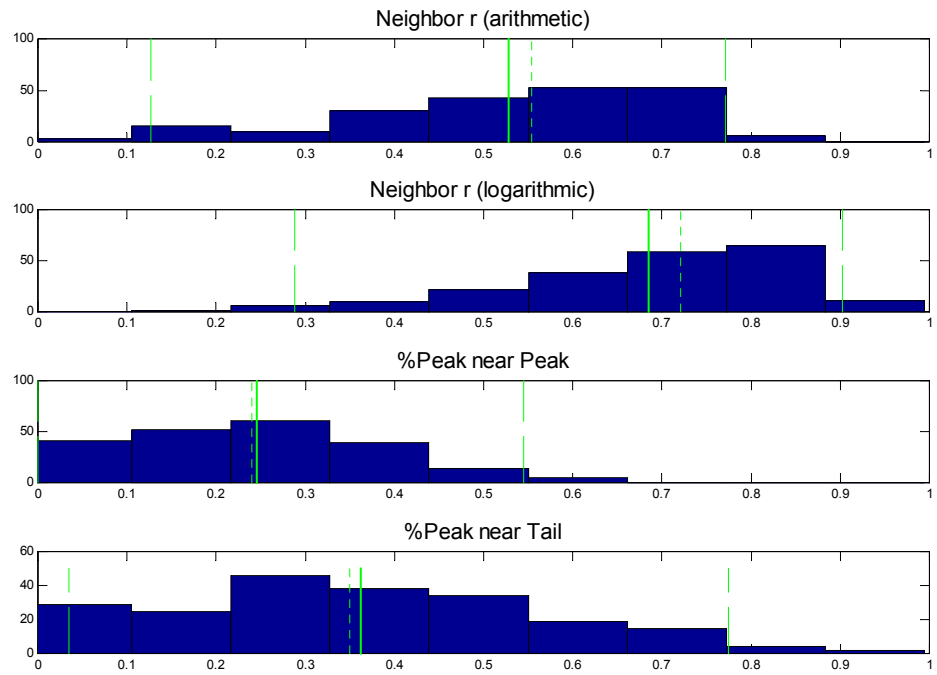
Figure 8 – Distribution of measures of smooth variation in abundances across a range for actual species ranges. These measures are as described in **Table 2**.
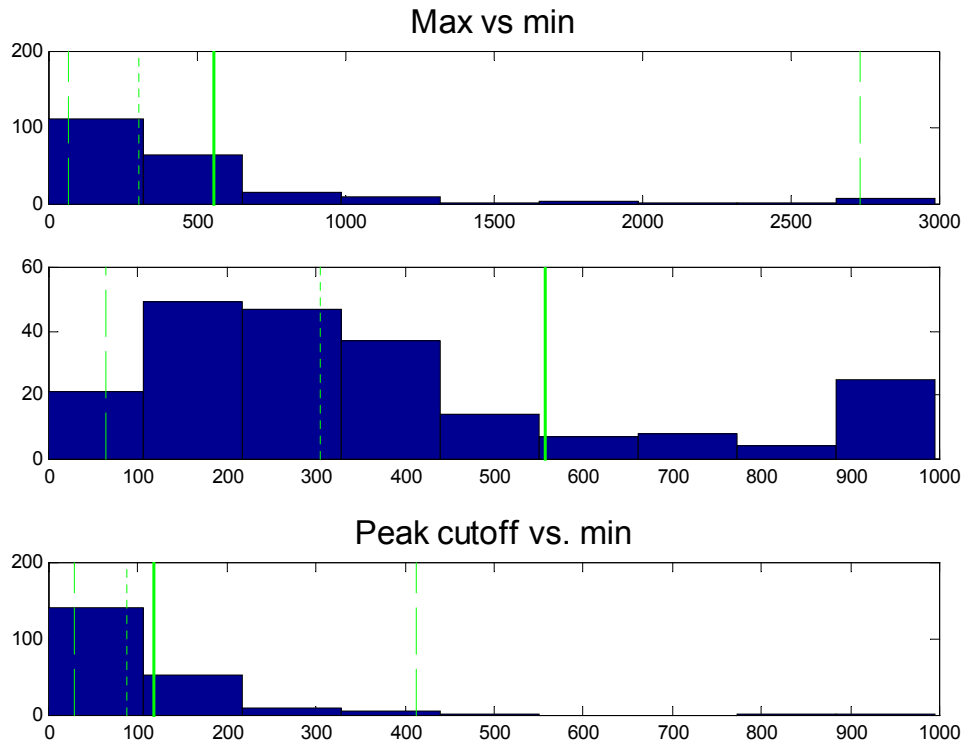
Figure 9 – measures of variation in contrast between peak abundances and tail abundances This diagram shows the distribution of ratios between peak abundances and tail abundances. The top figure shows the highest abundance observed for a species divided by the lowest abundance. The second figure shows the distribution just over the range 0-1000 (cases larger than 1000 appear in the 900-1000 bar). The "Peak cutoff vs. min" diagram shows the peak cutoff (70% of the maximum abundance on a log scale) vs. the minimum observed abundance.
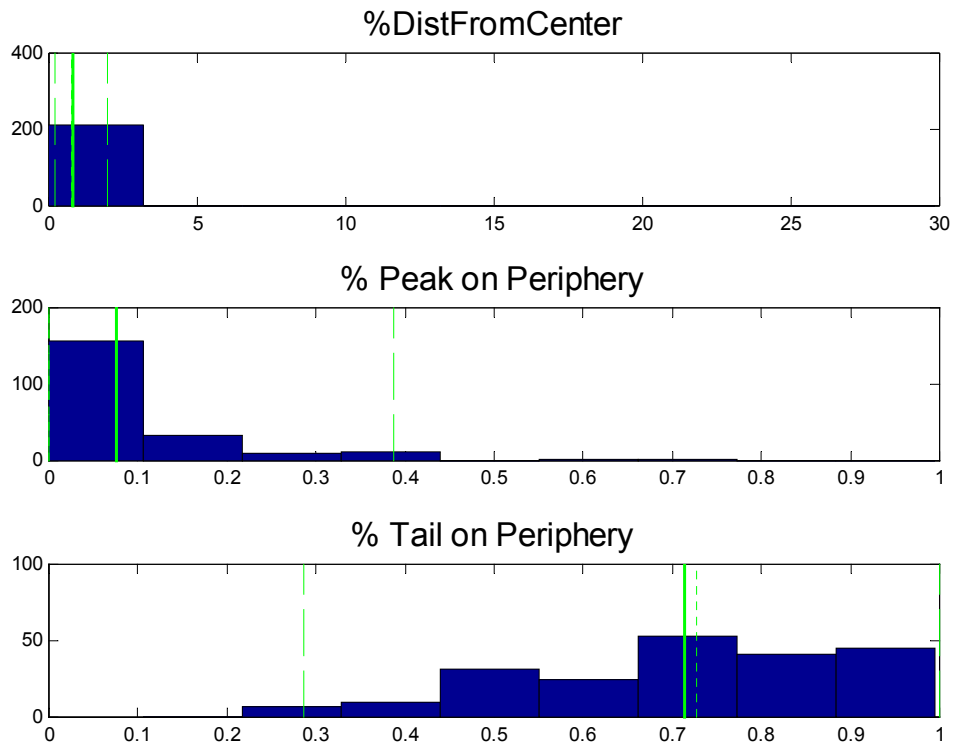
Figure 10- Distribution of measures of location of peak abundance relative to the center of the range for actual species ranges. : %DistFromCenter gives the distance of the highest peak in abundance from the center of the range calculated as a percentage of the range radius (square root of range area divided by π). The average is 0.813674 with 95% of values in the range (0.189666-1.98611) and a median of 0.748877. The periphery (of the convex hull, i.e the range boundary), consists on average of 7.5% peaks, and 71.4% tails which is quite close to the average over the whole range of 6.7% and 71.7% respectively.
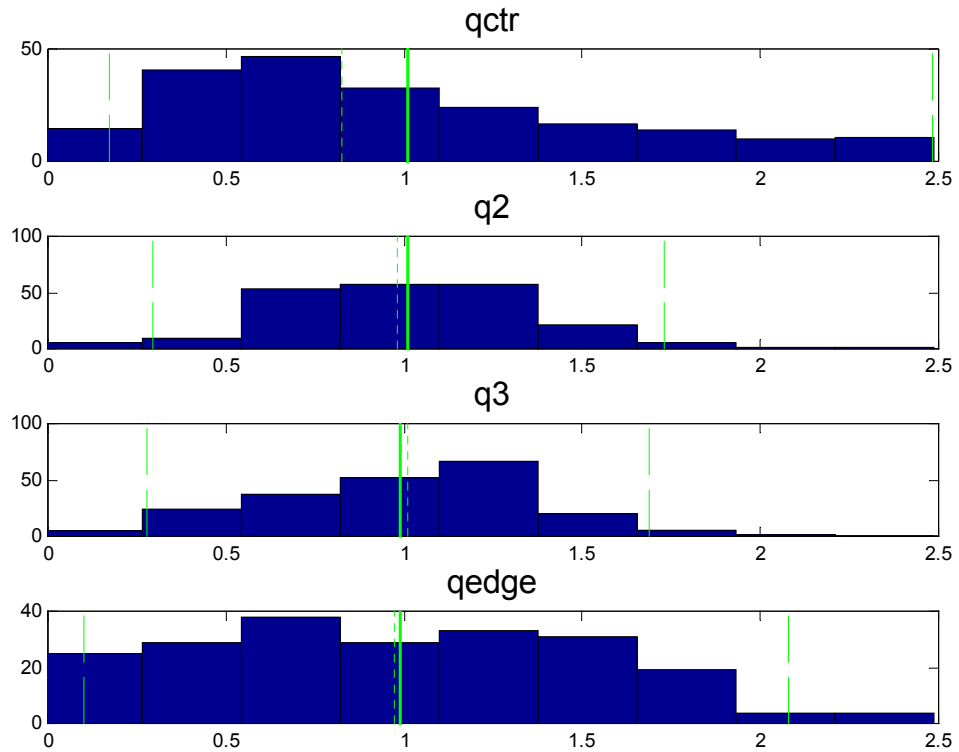
Figure 11 – measure of abundances for different portions of the range. Four

concentric rings were draw for each species range. QCTR contains the 25% of sites

furthest from the edge, while QEDGE contains the 25% closes to the convex hull range

boundary. Q2 is closer to the center than Q3. The abundance in each of these rings was

averaged and then divided by the average for the whole species. An index of 1 indicates

no deviation of a given ring from the average for the whole range. Although there is

considerable variation (presumably based on which ring contains the peak), on average

all four rings average within 0.01 of 1.0, indicating that all parts of a range have an equal

chance of containing high or low abundances.
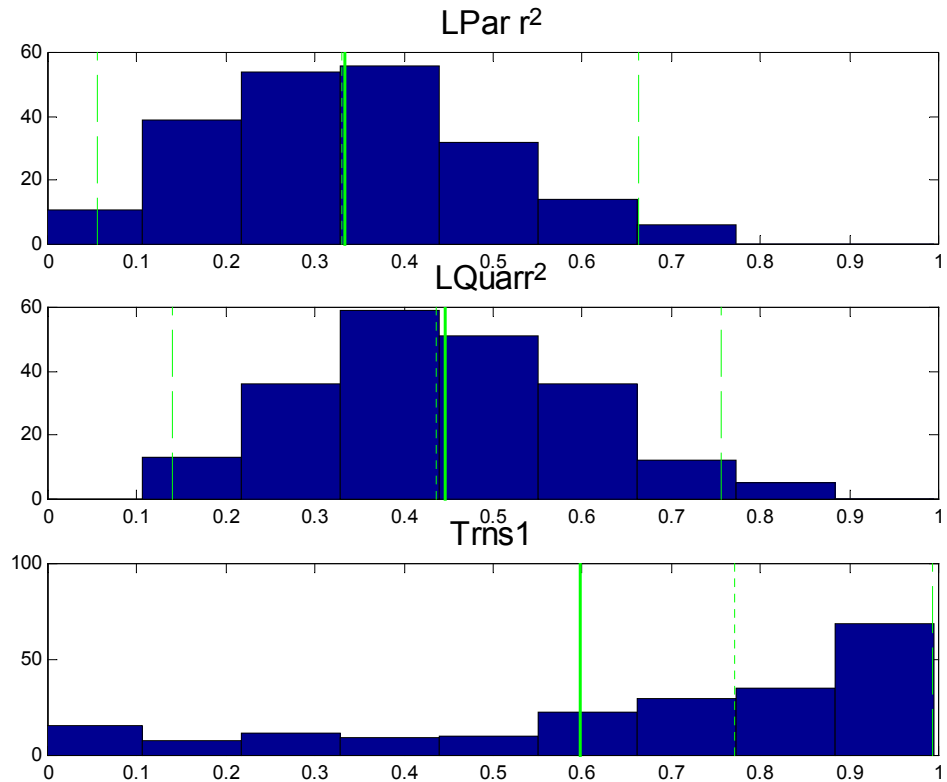
Figure 12 – Distribution of measures of goodness of fit of Gaussian and quasi-Gaussian functions to abundances of actual species ranges This figure gives the distribution for actual species ranges behind the averages reported in **Table 4**. **LPar r^2** gives the r^2 for log transformed data fitted by a parabola (equivalent to fitting a Gaussian surface in arithmetic space). Similarly, **Lquar r^2** gives the r^2 for fitting a quartic surface (polynomial of order 4). **Trns1** gives the r^2 for fitting a modified Gaussian function to a 1-Dimensional transect from the highest abundance to the farthest edge.
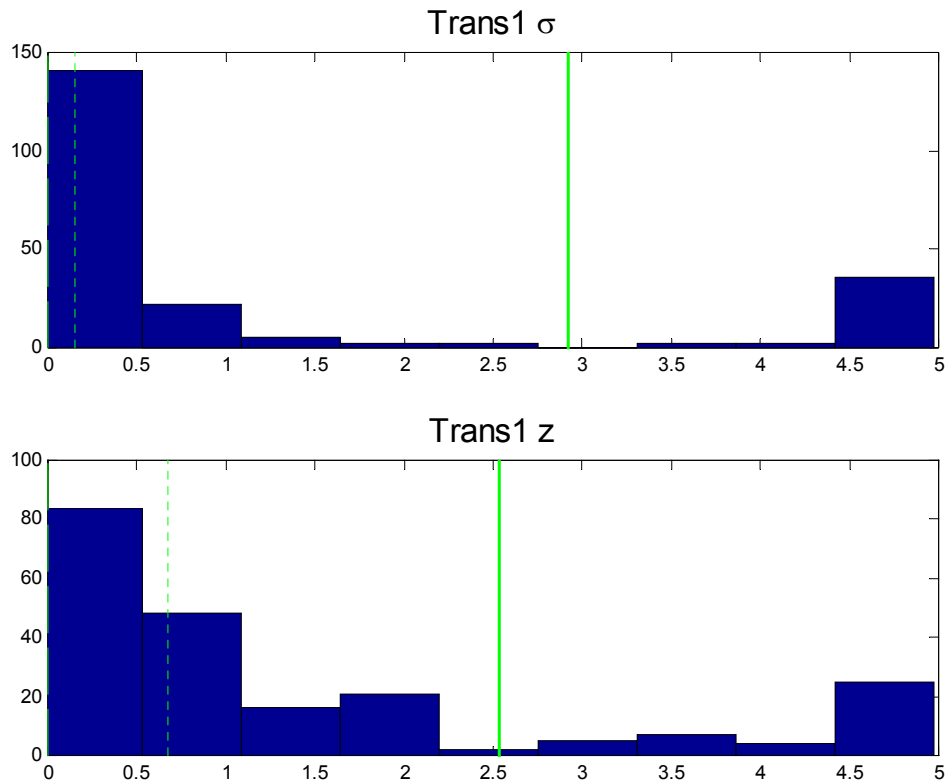
Figure 13 – Distribution of the shape of the modified Gaussian curve fit to a

1-D transect of data Trans1σ describes the width of the peaks. **Trans1z** describes the

rate of drop-off (z=2 matches the normal curve, while higher values are more

leptokurtic).
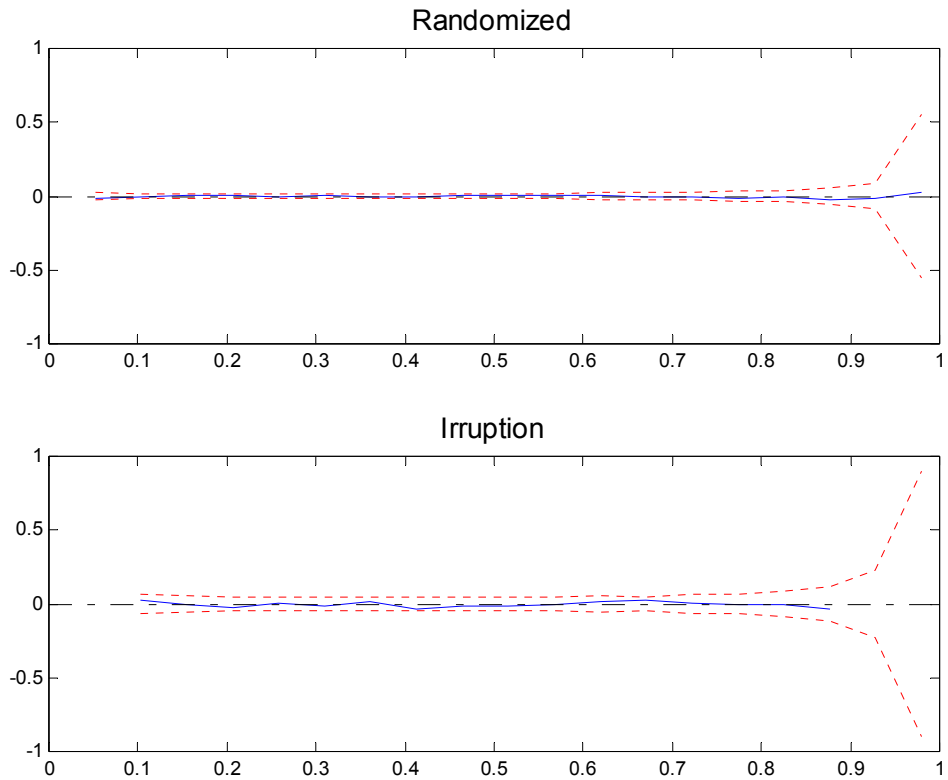
Figure 14 – Spatial autocorellograms for spatially randomized null models

The autocorrelograms for the four null models presented in Figure 3. The vertical axis gives a measure of correlation roughly analogous to Pearson's r, ranging from −1 to 1. The horizontal axis gives the distance between points (spatial lag), rescaled such that the greatest distance is 1. The paired dotted lines give a 95% confidence interval.
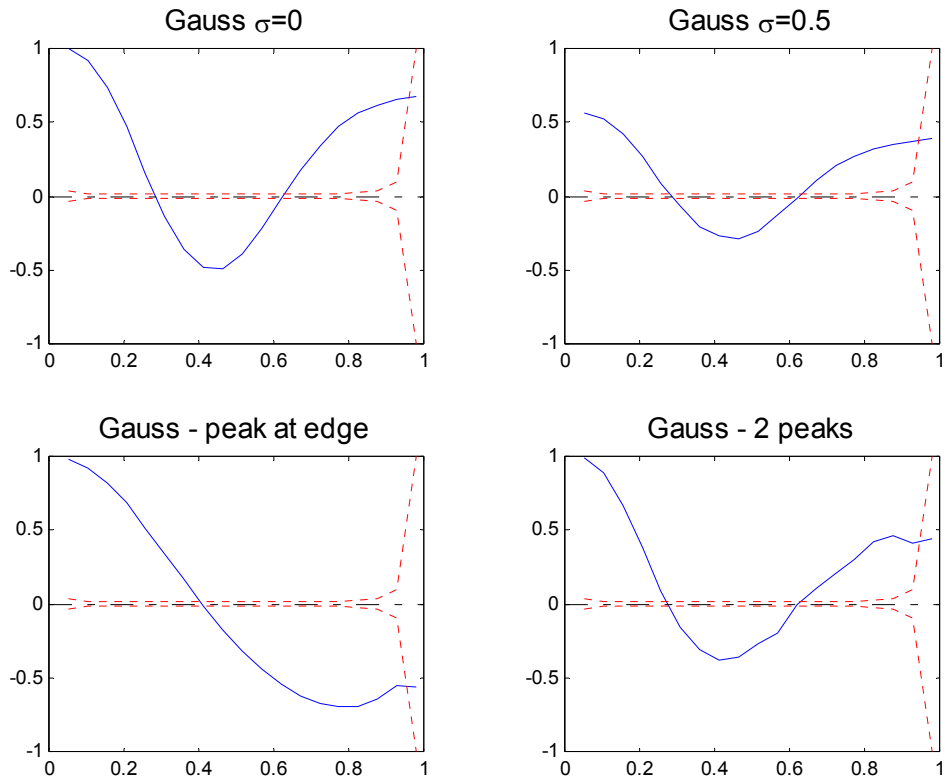
Figure 15 – Spatial autocorrelograms for Gaussian null models The autocorrelograms for the four null models presented in Figure 4. The vertical axis gives a measure of correlation roughly analogous to Pearson's r, ranging from −1 to 1. The horizontal axis gives the distance between points (spatial lag), rescaled such that the greatest distance is 1. The paired dotted lines give a 95% confidence interval.
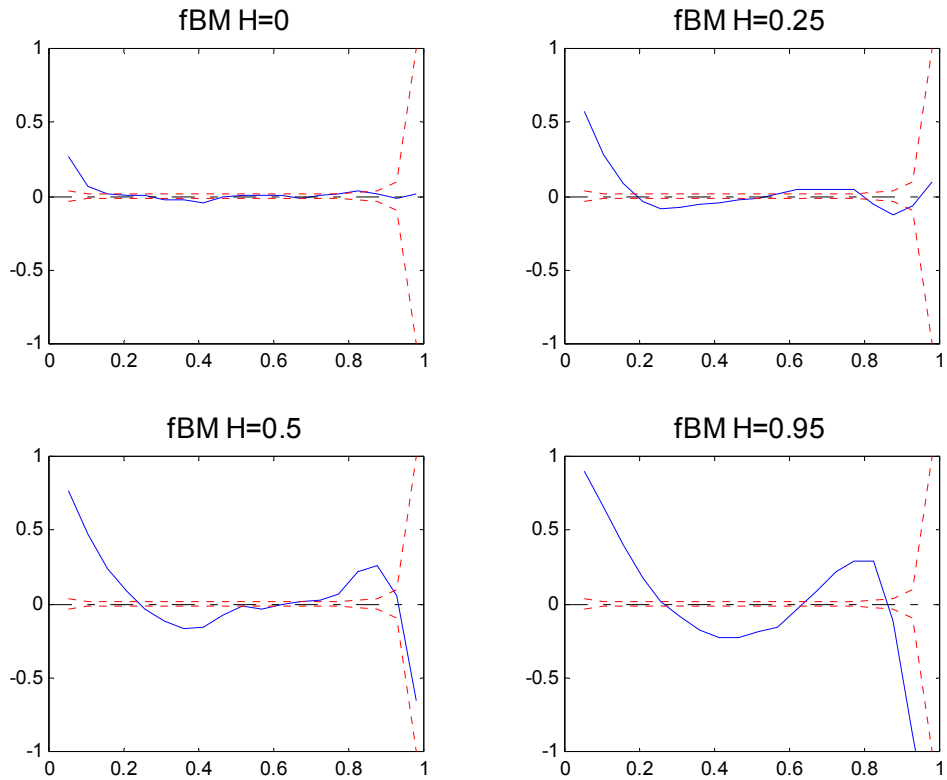
Figure 16 – Spatial autocorellograms for fBM nullmodels The autocorrelograms for the four null models presented in Figure 5. The vertical axis gives a measure of correlation roughly analogous to Pearson's r, ranging from −1 to 1. The horizontal axis gives the distance between points (spatial lag), rescaled such that the greatest distance is 1. The paired dotted lines give a 95% confidence interval.
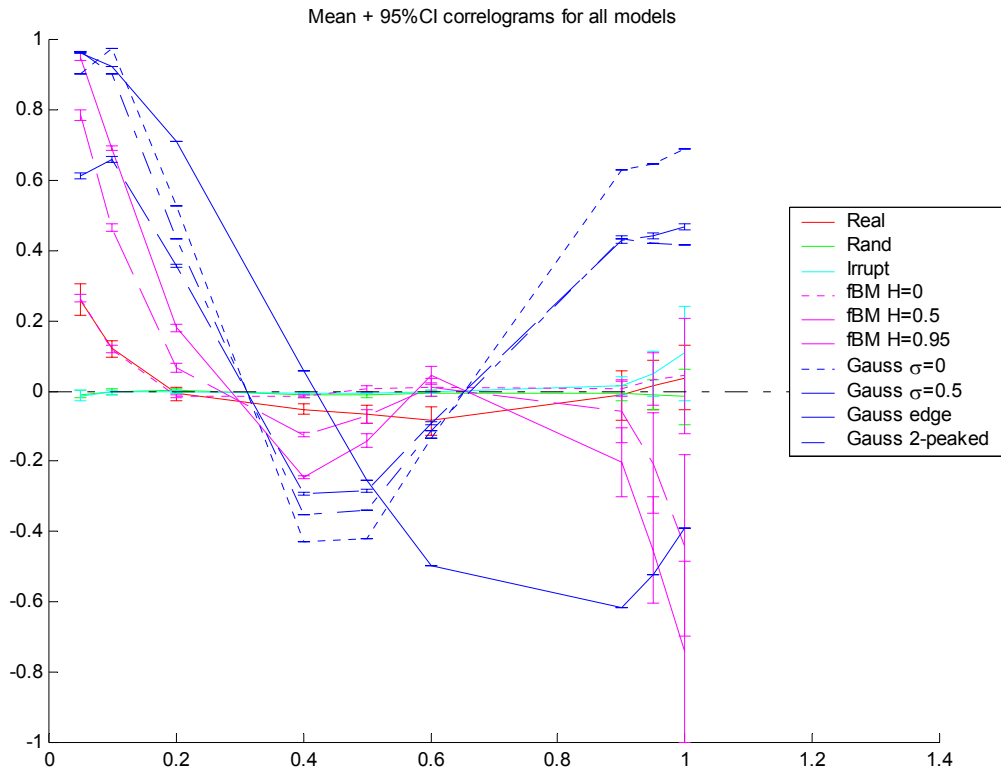
Figure 17 – Average spatial autocorrelograms for empirical data and null models. Most of these lines represent the average of 212 different spatial autocorrelograms. The errorbars denote one standard error. The interpretation of this figure is described in the text under the heading "**Results - Autocorrelation**".
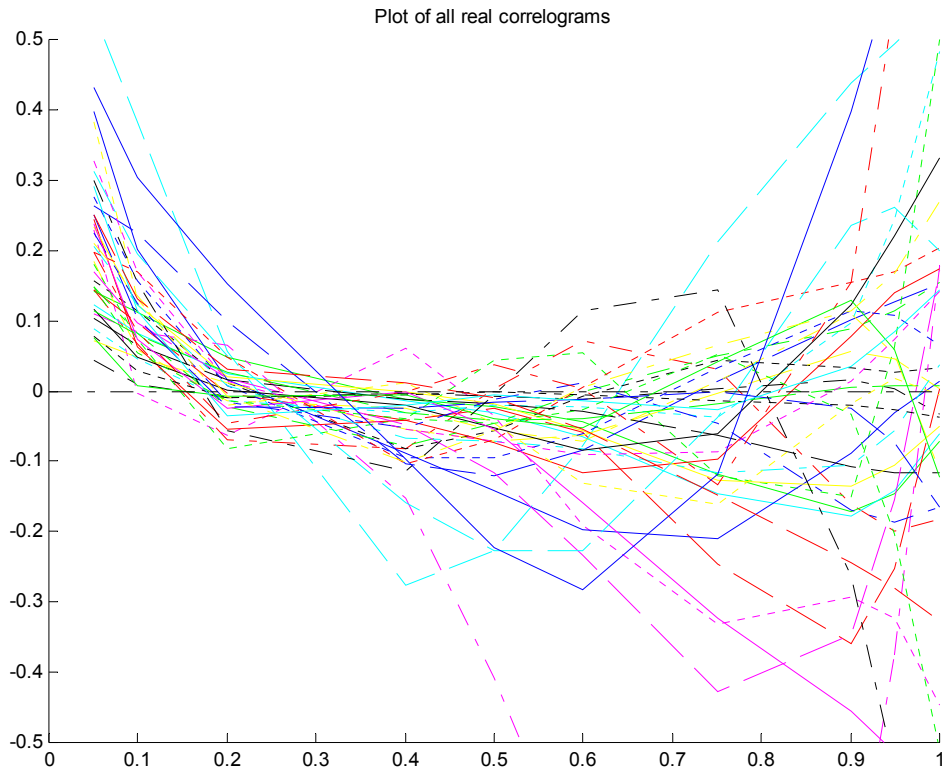
Figure 18- Sample of spatial autocorrelograms for empirical data This

diagram gives a random sample of 40 autocorrelograms for actual species SAASR data.

The interpretation is discussed in the text.
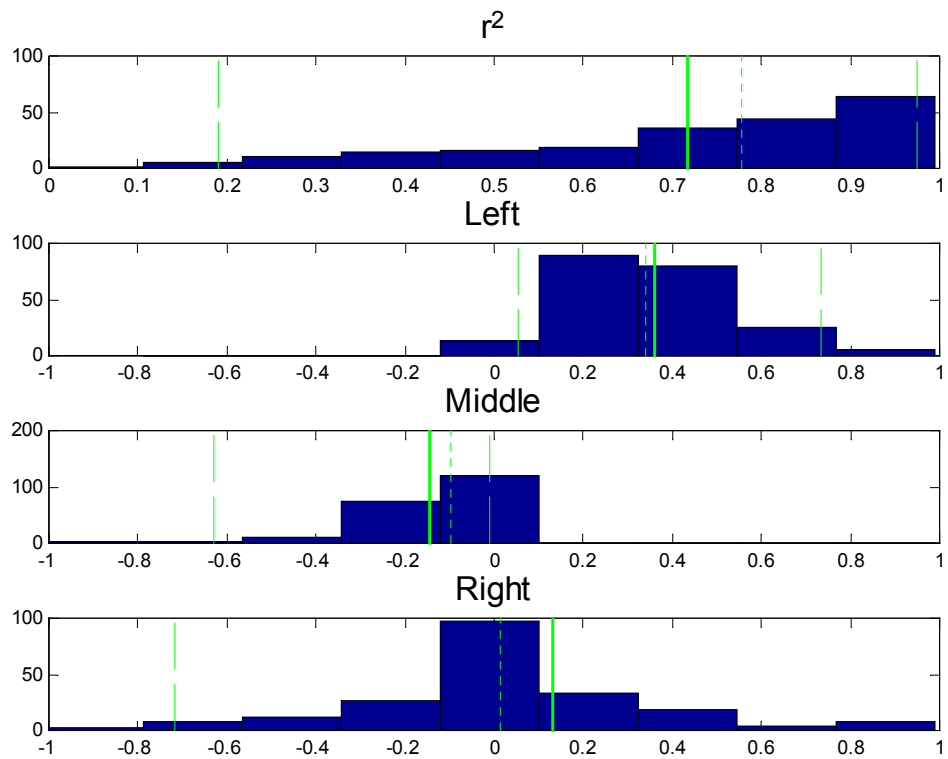
Figure 19 – Autocorrelation structure of empirical SAASR – This figure gives the distribution of the left, right, and middle (lowest point) correlation values for autocorrelograms calculated on 212 species of bird. This gives detail on data provided in Table 5.
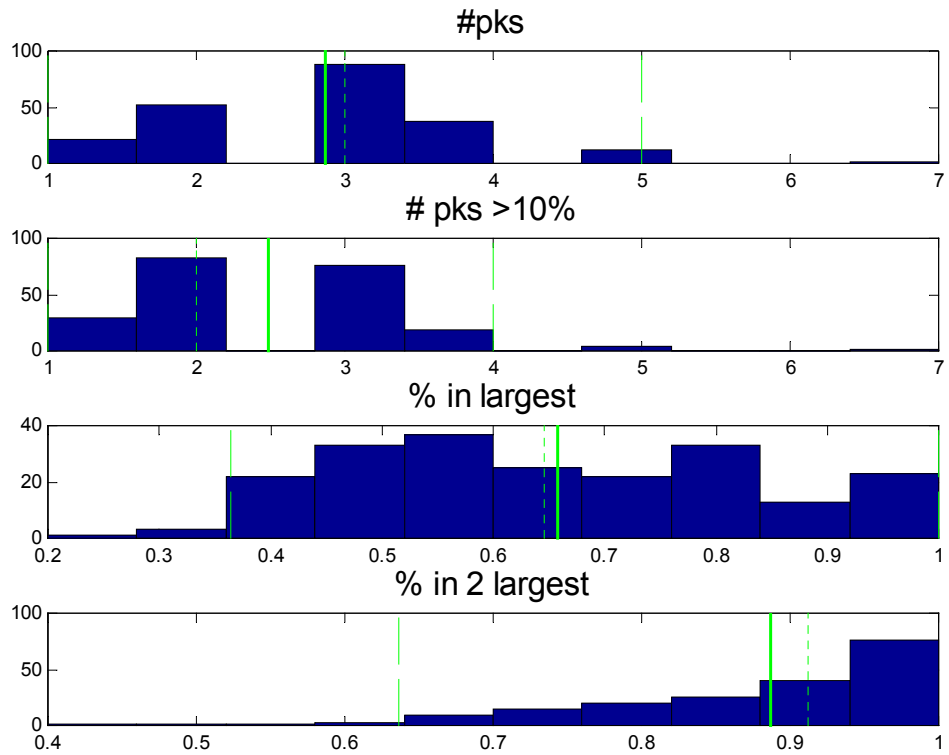
Figure 20 – Number of peaks This figure gives a histogram of data on the number of peaks in empirical species SAASRs. **#PKS** gives the number of peaks identified. **#PKS>10%** denotes only large peaks (peaks containing at least 10% as many routes as the largest peak for the species). **% in largest** gives the % of all peak routes which appear in the largest peak. **% in 2 largest** gives the % of all peak routes which appear in the two largest peaks for a given species.
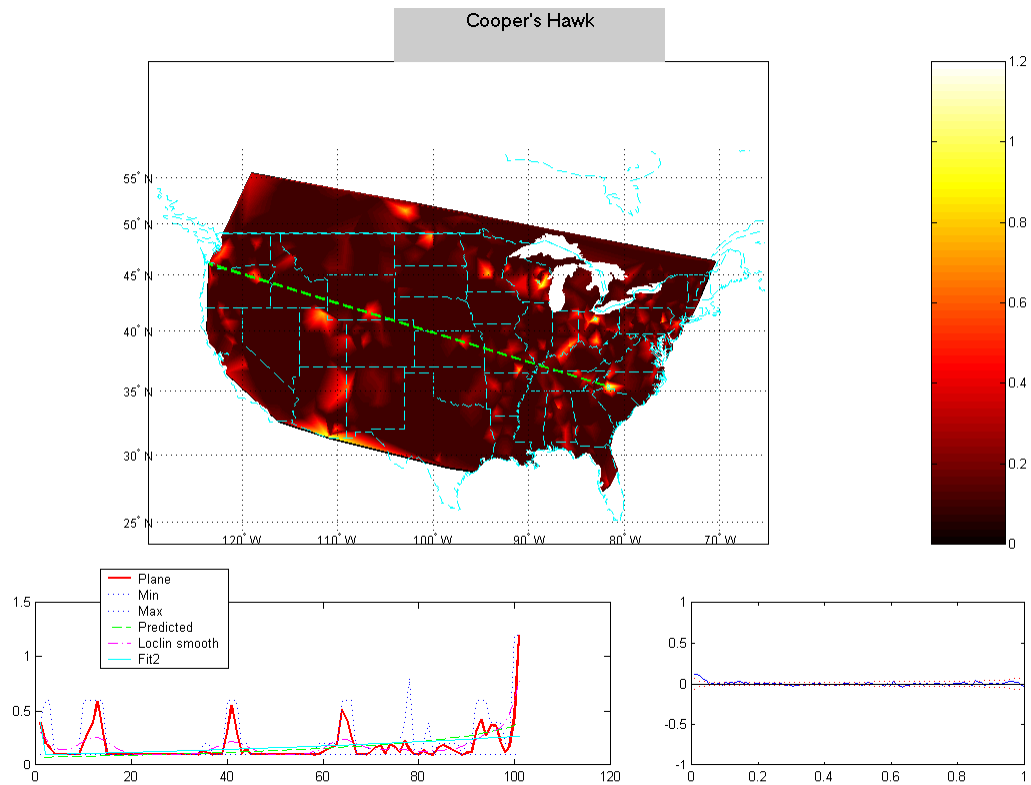
Figure 21 – Cooper's hawk This figures shows various aspects of the SAASR pattern for the species Cooper's hawk. Note the irruptive nature of the SAASR pattern. The top left figure gives a map of species abundances observed in the BBS. Lighter colors represent higher abundances as denoted by the colorbar to the right. The thick dashed line denotes a transect taken from the highest abundance to the farthest away corner. The bottom left figure gives abundances along this transect. The thick red line represents the locally interpolated values. The two dotted lines indicates the maximum and minimum abundance which were used in interpolating this value (out of the three points used). The dashed line shows the abundances predicted by fitting a modified Gaussian function. The smooth solid line shows the abundances predicted by fitting a combination of two Gaussian functions. The figure at the bottom right gives the autocorrelogram for this species.
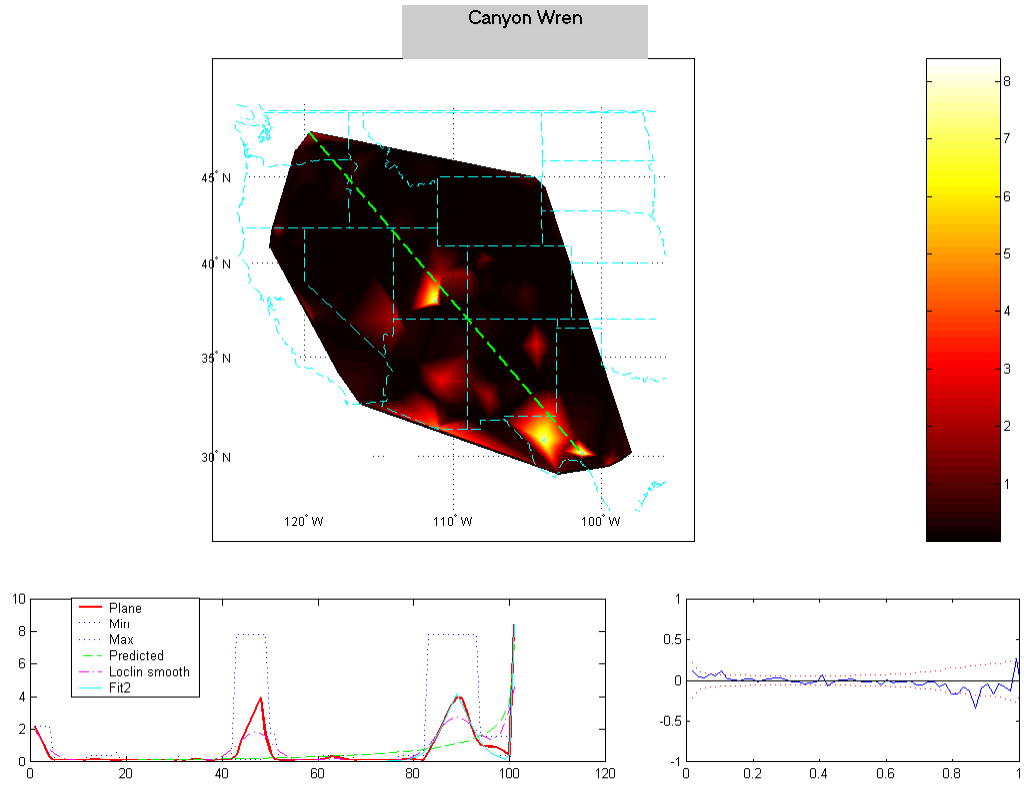
Figure 22 canyon wren As for Figure 21 but for the canyon wren. Note the irruptive nature of the SAASR pattern.
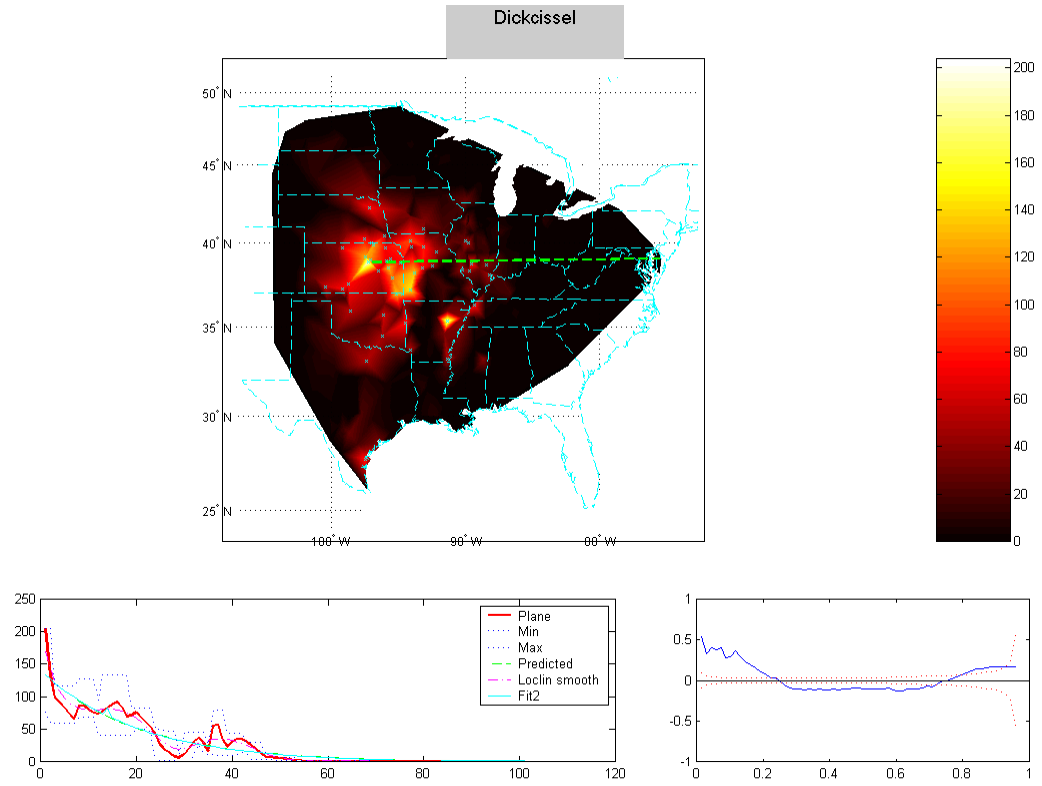
Figure 23 dickcissel As for Figure 21 but for the dickcissel. Note the nearly

Guassian nature of the SAASR pattern (albeit with noise).
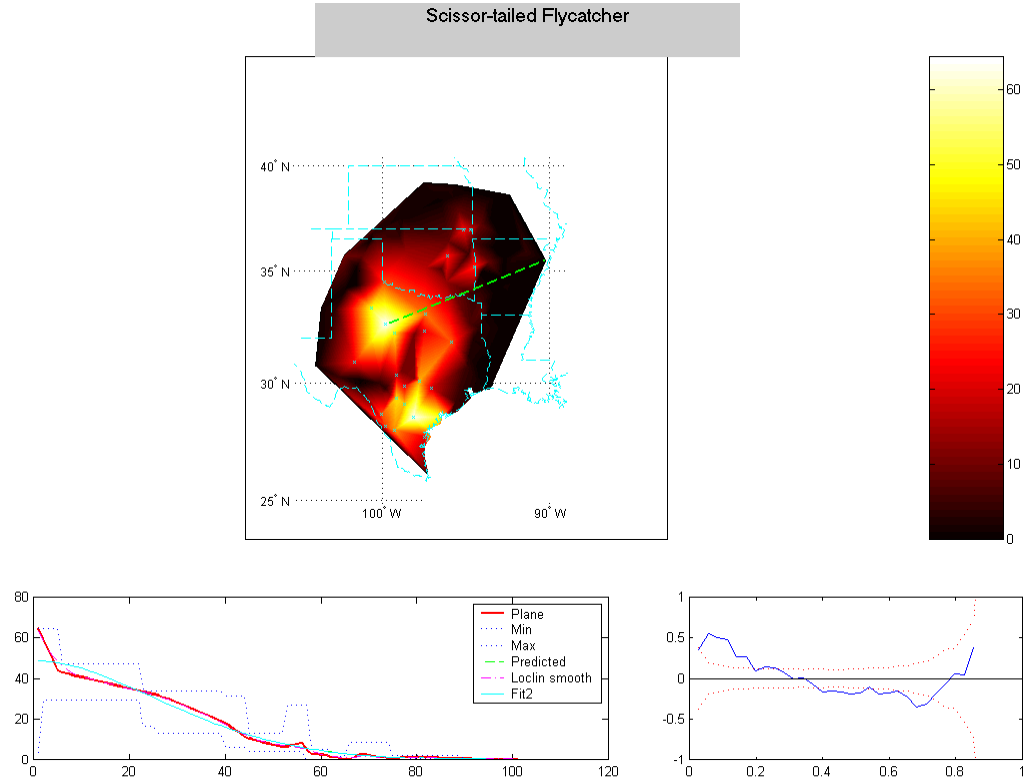
Figure 24 scissor-tailed flycatcher As for Figure 21 but for the scissor-tailed flycatcher. Note the nearly Guassian nature of the SAASR pattern (albeit with noise).
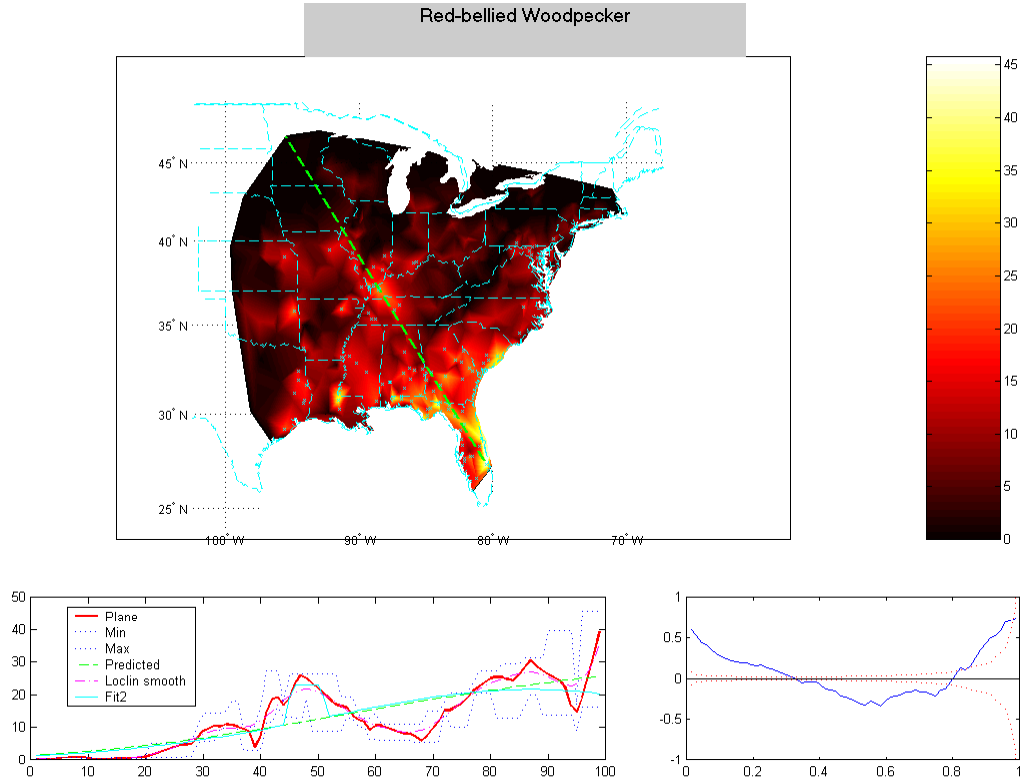
Figure 25 Red-bellied Woodpecker As for Figure 21 but for the Red-bellied

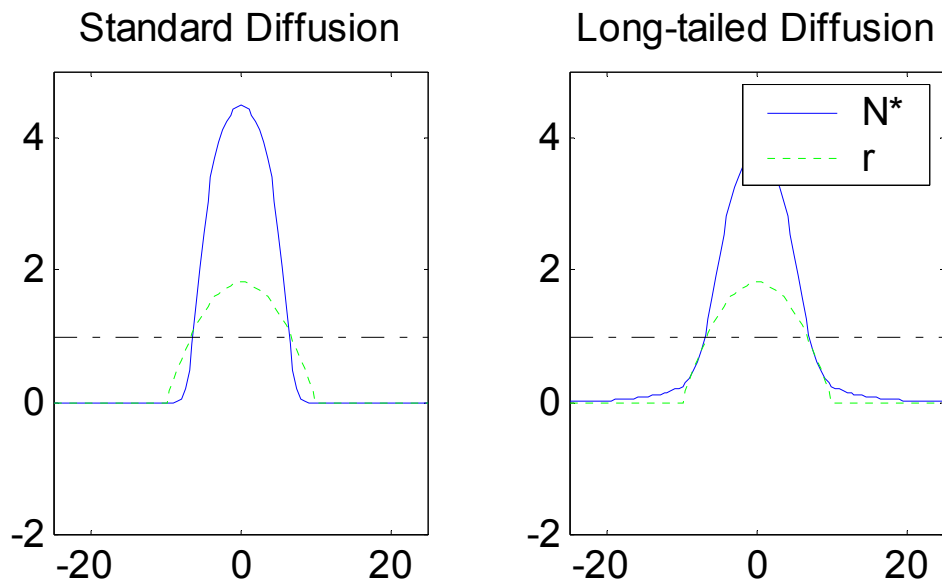woodpecker. Note that the SAASR is intermediate between irruptive and Gaussian.

Figure 26 – Comparison of diffusion models This figure shows the output from two simulations of diffusion. The dotted line shows the physiological response surface (fitness). The solid line shows equilibrium abundances across space. The dash-dot line shows fitness = 1 (constant population size). The figure on the left shows traditional, local diffusion. The right figure is identical but it shows the results of heavy-tailed diffusion. This figure clearly has a tail in abundance with a source-sink dynamic.
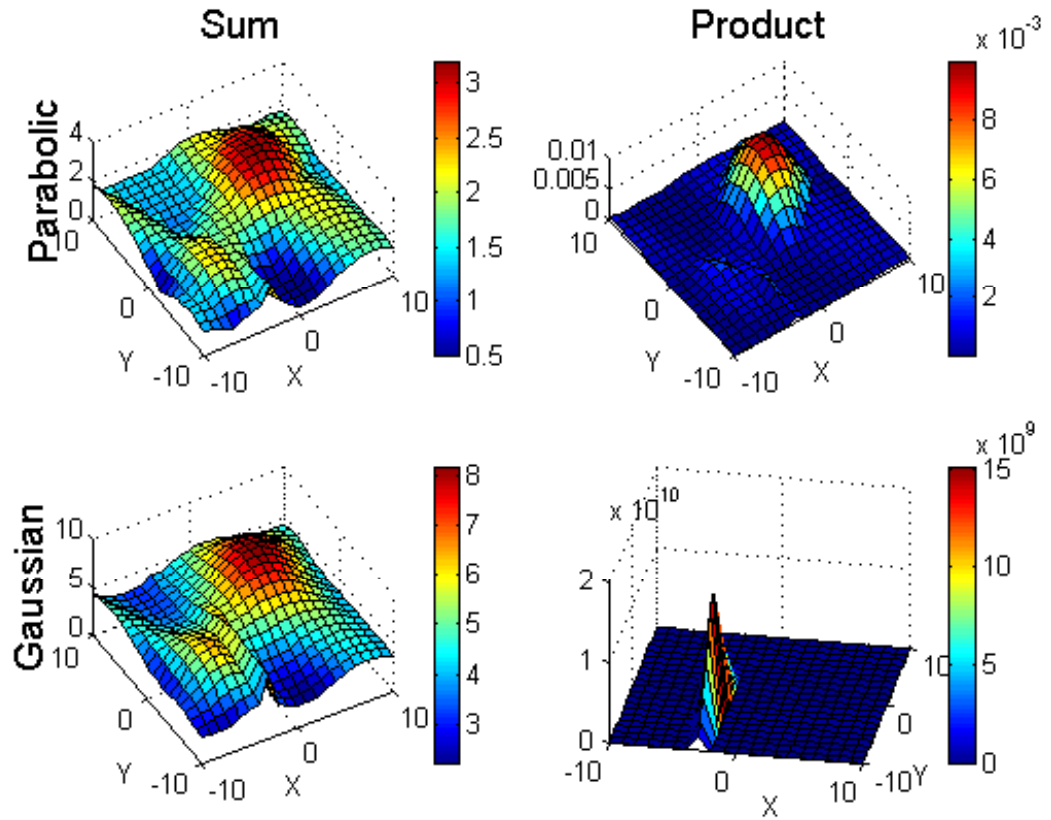
Figure 27 – Tests of Brown's niche hypothesis model of SAASRs Abundance surfaces (SAASRs) for four variations of Brown's model. The top row has a parabolic fitness response surface, the bottom row has a Gaussian response surface. The left column uses an additive model. The right column uses a multiplicative model.
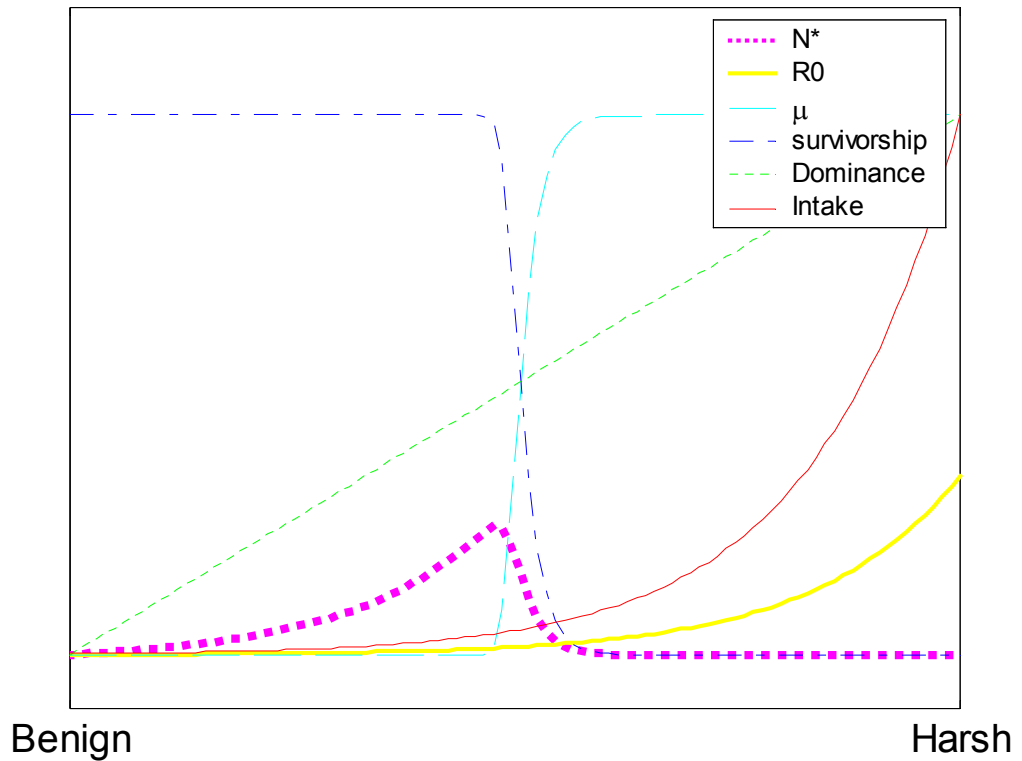
Figure 28 – Tradeoff along gradient model of SAASR Output from calculations of a model presented in the text for tradeoffs in environmental tolerance and competitive tolerance along a gradient. The thick dotted line shows equilibrium abundance across the gradient (N*). The two sigmoidal dashed lines show survivorship and mortality. The straight dotted line shows dominance. The two solid exponential-shaped lines show intake (which is a function of dominance) and the fecundity which is a linear function of intake. N* is the product of fecundity and survivorship.